

Enigmatic Glass-Like Carbon from the Alpine Foreland, Southeast Germany: A Natural Carbonization Process

Tatyana G. SHUMILOVA^{1,2}, Sergey I. ISAENKO¹, Vasily V. ULYASHEV¹, Boris A. MAKEEV¹, Michael A. RAPPENGLÜCK³, Aleksey A. VELIGZHANIN⁴ and Kord ERNSTSON^{5,*}

1 Institute of Geology of Komi Scientific Center of Ural Branch of Russian Academy of Sciences, Pervomayskaya st. 54, Syktyvkar, 167982, Russia

2 Hawaii Institute of Geophysics and Planetology, University of Hawaii at Manoa, 1680 East-West Road, Honolulu, HI, 96822, USA

3 Institute for Interdisciplinary Studies, Gilching, Germany

4 National Research Center «Kurchatov Institute», Akademika Kurchatova pl. 1, Moscow, 123182, Russia

5 Faculty of Philosophy I, University of Würzburg, Germany

Abstract: Unusual carbonaceous matter, termed here *chiemite*, composed of more than 90% C from the Alpine Foreland at Lake Chiemsee in Bavaria, southeastern Germany has been investigated using optical and atomic force microscopy, X-ray fluorescence spectroscopy, scanning and transmission electron microscopy, high-resolution Raman spectroscopy, X-ray diffraction and differential thermal analysis, as well as by $\delta^{13}\text{C}$ and ^{14}C radiocarbon isotopic data analysis. In the pumice-like fragments, poorly ordered carbon matter co-exists with high-ordering monocrystalline α -carbyne, and contains submicrometer-sized inclusions of complex composition. Diamond and carbyne add to the peculiar mix of matter. The required very high temperatures and pressures for carbyne formation point to a shock event probably from the recently proposed Holocene Chiemgau meteorite impact. The carbon material is suggested to have largely formed from heavily shocked coal, vegetation like wood, and peat from the impact target area. The carbonization/coalification high PT process may be attributed to a strong shock that instantaneously caused the complete evaporation and loss of volatile matter and water, which nevertheless preserved the original cellular structure seen fossilized in many fragments. Relatively fresh wood encapsulated in the purported strongly shocked matter point to quenched carbon melt components possibly important for the discussion of survival of organic matter in meteorite impacts, implying an astrobiological relationship.

Key words: astrobiology, diamond, carbyne, coalification, carbonization, meteorite impact, *chiemite*

1 Introduction

In nature carbon is commonly known to form crystalline structures like graphite, diamond, and more rarely, lonsdaleite, a hexagonal diamond allotrope, and chaoite; as well there are shungite, a low-ordered glass-like carbon, and carboniferous substances – coals and soot. In the last decades a further form, fullerenes, a naturally occurring carbon allotrope in diverse molecular variants has been established. Fullerenes and more carbon allotropes have increasingly attracted attention in laboratory work and in industry because of their in-part exceptional properties,

and many other possible forms have been predicted theoretically and experimentally produced (e.g., Terrones et al. 2000; Correa et al. 2006; Itoh et al. 2009; Tagami et al. 2014; Lin et al. 2011; Narayan, and Bhaumik 2015).

A special group of diamond carbon has in the past attracted attention because of the occurrences in impact structures (e.g., Popigai crater in Masaitis et al. 1972; Ries crater in El Goresy et al. 2001, 2003), where a shock-produced transition from graphite has been established. As early as the 1980s, diamond formation from organic matter in sedimentary rocks has occasionally been addressed for the Kara impact structure, at Pay-Khoy, Nenetsia and Khanty-Mansia, Russia, but only recently has the post-coal carbon-diamond transition at Kara been

* Corresponding author. E-mail: kernstson@ernstson.de

analyzed using modern high-resolution methods to reveal new insights into the mechanism of formation and special properties (Shumilova et al. 2018, and references therein).

Here we report on an unusual carbonaceous matter from a limited region in southeast Bavaria, which contains diamond and the rare carbon allotrope carbyne (e.g., Castelli et al. 2012; Liu et al. 2013; Pan et al. 2015) (Fig. 1). The matter has attracted increased interest in the last decade (e.g., Isaenko et al. 2012), although it had been known for some time without anyone giving it further consideration mostly because of a confusion with coke fragments on very cursory inspection. It finally appeared conspicuous to a group of local history researchers and experienced amateur archaeologists when they found that the several fragments frequently strongly disturbed their metal detectors because of the considerable electrical conductivity. They began to doubt the coke explanation because they were unable to inflame these fragments, which, although friable, surprisingly could only be sawed through with a diamond blade.

The matter in the fragments was basically unknown from any industrial or other anthropogenic processes, although the porous texture resembles that of activated coal. Hence, the amateur researchers concluded that the matter could have originated from a previously unknown natural process, which was underlined by samples found on a small island in the large Lake Chiemsee (Fig. 1) and at some altitude in the pre-Alps mountains.

For this first thorough investigation of the matter, which strengthens the idea of an origin from an unusual natural process, we here term the substance *chiemite*, as a working

name based on its first occurrence in the Chiemgau district.

2 Chiemite Location and Description

The carbon-based chiemite exhibits as a black glass-like matter with a highly porous structure and a greasy luster. The material is found scattered in the field as rounded to subrounded pebbles and cobbles and also as smaller irregular fragments (Fig. 2a). Some cobbles sampled appear to have been shaped aerodynamically as they exhibit flow texture (Fig. 2c), and, in one case, a sandstone cobble from Lake Chiemsee in Bavaria in part shows a coating with a chiemite crust (Fig. 2d). Occasionally, chiemite appears pseudomorphic after wooden fragments of branches (Fig. 2b). A very thin grayish skin is mostly observed, which is frequently covered by a whitish carbonate crust. A brownish surficial color might be due to muddy or loamy impregnation (Fig. 2a, b). Freshly crushed surfaces exhibit an inky-black color and a glassy to metallic luster (Fig. 3a). The texture of the pieces can vary significantly. We observe a strongly vesicular, pumice-like interior wherein a few, mostly platy-black inclusions are sticking (Fig. 3a), and various transitions to more dense and platy pieces, and even a tabular, porous and platy, texture may occur. Frequently, the platy inclusions show obvious charcoal displaying partly fibrous texture (Fig. 3b) whereas their color and luster do not differ from the porous, pumice-like parts. Less frequently, chiemite with encapsulated fresh wood particles (Fig. 3c) and brecciated specimens (Fig. 3d) occur.

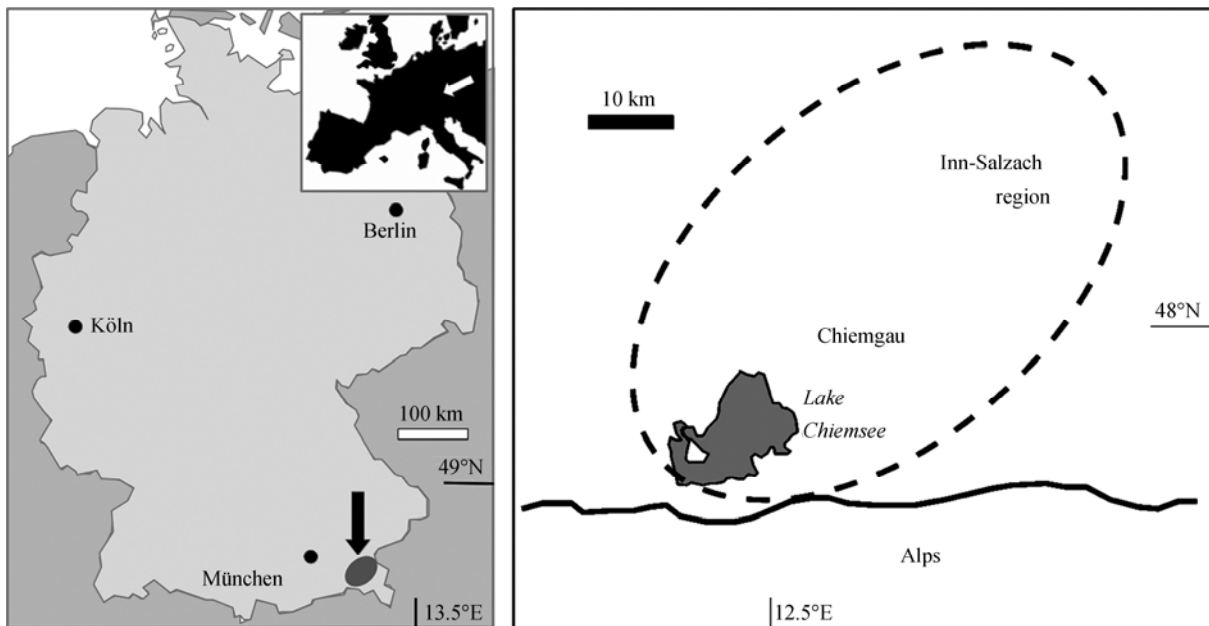


Fig. 1. Location maps. To the right, the ellipse roughly outlines the Chiemgau meteorite impact crater strewn field. The chiemite samples are widely distributed in this area with some concentration on the Lake Chiemsee shore.



Fig. 2. (a), Smaller chiemite pieces sampled from the field; (b), larger chiemite fragments pseudomorphic after pieces of branches, centimeter scale; (c), an aerodynamically shaped chiemite piece with flow texture; (d), chiemite crust on a sandstone cobble (inserted image) from Lake Chiemsee, long side = 12 cm. Pinheads = 2 mm.

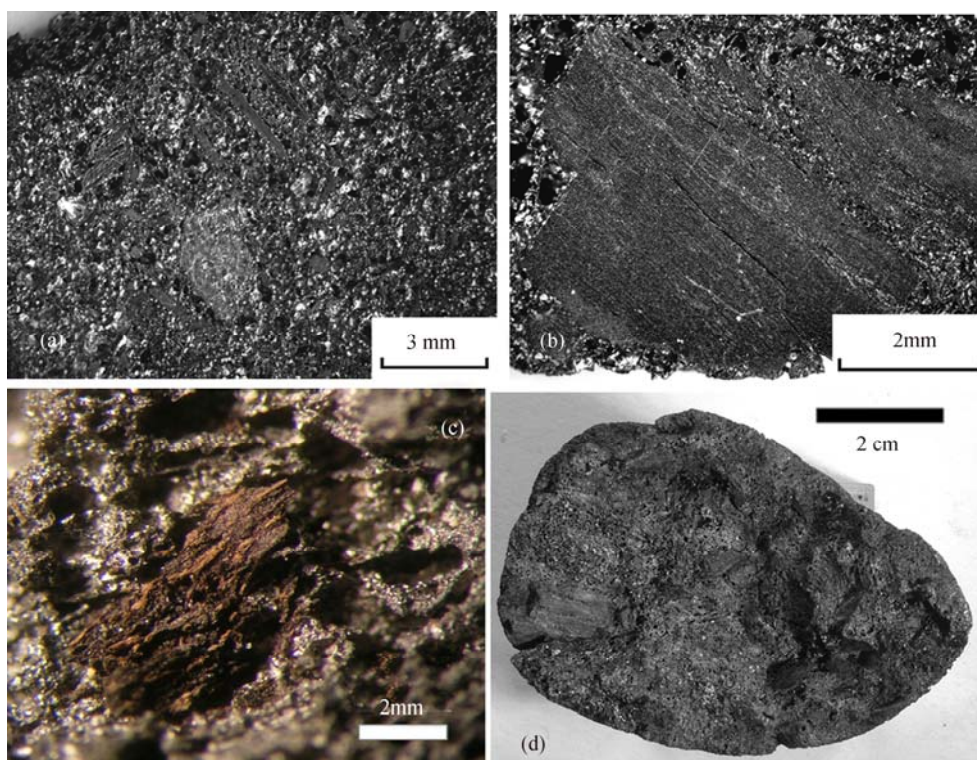


Fig. 3. Visual aspects of chiemite samples.

(a), Freshly broken chiemite sample exhibiting platy inclusions in a vesicular matrix. (b), detail showing fossilized wooden structure. (c), relatively fresh wood particle embedded in chiemite. (d), chiemite pebble with a breccia texture.

Depending on differences in the porous structure the density varies but in most cases, is $<1 \text{ g/cm}^3$, i.e., the pieces with few exceptions can float on water. This may explain why quite a few well-rounded chiemite pebbles and cobbles are found on the shore of Lake Chiemsee. We measured resistivity and magnetic properties in somewhat larger samples. The resistivity proved to be widely homogeneous having low values between 0.01 and 0.015 $\text{Ohm}\cdot\text{m}$. Magnetic susceptibility ranged roughly between $+0.5\cdot 10^{-3}$ and $+0.8\cdot 10^{-3}$ SI, while remnant magnetizations showed stronger variation, between negligible and about maximum 0.1A/m, implying Koenigsberger ratios of up to 2. Carbon modifications in general show a diamagnetic behavior; however, the chiemite remnant magnetization points to a content of ferromagnetic or/and ferrimagnetic matter. Coke for comparison shows a negligible magnetic susceptibility, usually near zero.

3 Methods and Sample Preparation

Four samples from different locations in the Chiemgau district were studied in detail at the Collective Use Center GEOSCIENCE (IG Komi SC UB RAS, Syktyvkar, Russia) with the following methods: optical and atomic force microscopy (AFM), X-ray fluorescence spectroscopy (XRF), scanning electron microscopy (SEM), microprobe analysis (MPA), transmission electron microscopy (TEM), high-resolution Raman spectroscopy (RS), infrared spectroscopy (IR), X-ray diffraction (XRD) and differential thermal analysis (DTA), as well as $\delta^{13}\text{C}$ studies. We should emphasize that, apart from XRF, the analyses have been applied to the more homogeneous, porous parts of the samples (Fig. 4), which are different

from the platy inclusions and appear to be representative of the matter.

Radiocarbon isotopic studies were provided at the Laboratory of Radiocarbon dating at the Institute of Geography RAS (Moscow, Russia). X-Ray synchrotron studies have been provided at the Kurchatov Institute (Moscow, Russia). To further understand the structural nature of the material, the chiemite samples were in some cases analyzed in comparison with poorly structured carbon substances—shungite (Shun'ga deposit, Russia), glass-like carbon (SU-2000, Novocherkassk factory production, Russia) and coal (Severnaya mine, Russia), which, however, are only peripherally referred to in this study.

First of all, unpolished freshly crushed pieces of the material were analyzed by optical microscopy in reflected nonpolarized light. This preliminary analysis served for the preparation for high-resolution methods. The element content impurities in a large volume were provided for crushed powder chiemite specimens by X-ray fluorescence spectroscopy with use of a fluorescence analyzer MESA-500 (Horiba). Structural features of the chiemite were analyzed by powder X-ray diffraction using an X-ray diffractometer XRD-6000 (Shimadzu, Japan) with Cu X-ray tube. X-ray powder diffraction was provided using a diffractometer Shimadzu XRD-6000 for the diapason $2\theta=2-120^\circ$. High-resolution X-Ray diffraction has been performed at the Structural Materials Science station of the Kurchatov synchrotron radiation source (Chernyshov et al. 2009) with FujiFilm Imaging Plate as the 2-D detector for the diffraction: exposure time was 20 minutes; X-ray wavelength equals to 0.104 nm was utilized; the beam size at the sample was $200\times 200 \mu\text{m}^2$; sample to detector

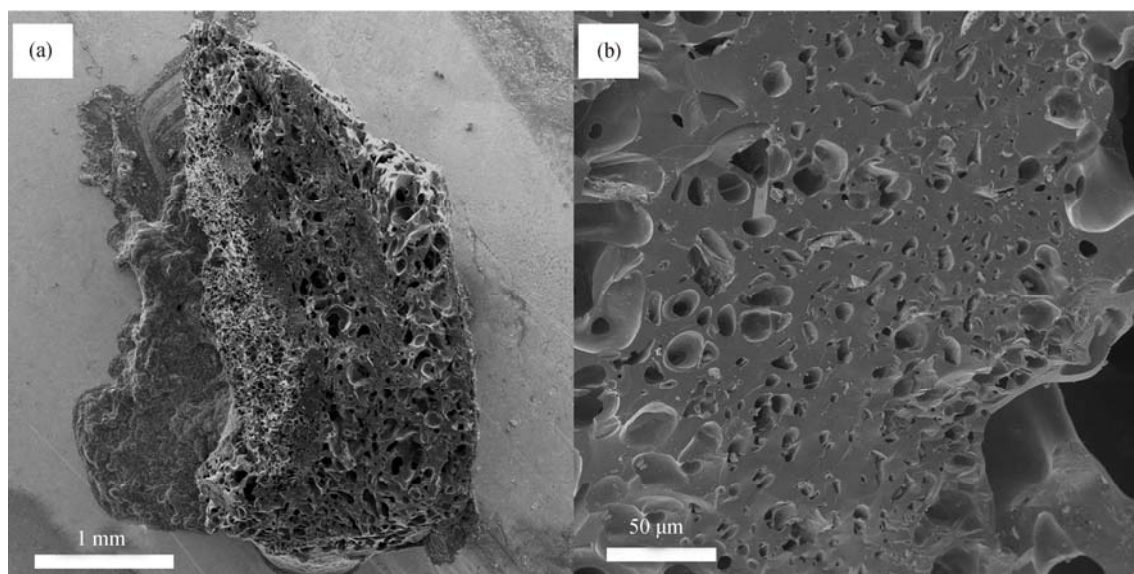


Fig. 4. SEM images of the chiemite matter; homogeneous part of a freshly broken fragment, Specimen 2009-2 (a) and magnified region (b).

distance was 118 mm. To refine sample-to-detector distance the NACF standard was utilized (Courbion and Ferey 1988). The powdered specimens were fixed on 'kapton' tape with an adhesive layer. Background data of the supporting material were subtracted from sample diffractograms. Two-dimensional diffraction data were integrated to $I(2\theta)$ form by the Fit2D program (Hammersley, 2016).

Electron microscopy and microprobe analysis was conducted on unpolished freshly crushed surfaces with a VEGA 3 TESCAN microscope (Czech Republic) combined with an energy-dispersive spectrometer and a detector (X-Max EDS, Oxford instruments) without conductive covering. TEM studies were provided with a transmission electron microscope TESLA BS-500.

All specimens are kept at the Institute of Geology of Komi Scientific Center (Dr. Shumilova).

4 Results

4.1 X-ray fluorescence spectroscopy

The chiemite samples consist mostly of carbon (Table 1).

Table 1 X-Ray fluorescence spectroscopy data

Chemical component	Chemical component content, mas. (%)			
	Kd-2006-1	Kd-2009-2	Kd-2010-4	Kd-2011-1
SiO ₂	4.64	4.35	2.86	4.24
TiO ₂	0.10	0.09	0.06	0.10
Al ₂ O ₃	2.58	2.77	1.87	2.54
Fe ₂ O ₃ total Fe	1.16	0.48	0.13	0.84
MnO	0.012	0.101	0.004	
MgO	0.26	0.47	0.19	0.57
CaO	0.19	2.18	0.19	0.28
K ₂ O	0.27	0.19	0.17	0.15
P ₂ O ₅		0.95	0.12	0.15
SO ₃ total S	0.77	0.36	0.41	1.13
NiO	0.004		0.003	
SrO	0.002	0.055		0.006
ZrO ₂				
C	90.00	88.00	94.00	90.00
Sum	100.00	100.00	100.00	100.00

The chemical components sum mass was calculated to 100 mas. (%); C content was estimated by thermal differential gravimetry analysis.

Table 2 X-Ray fluorescence spectroscopy data of the non-carbon content

Chemical component	Chemical component content, mas (%)			
	Kd-2006-1	Kd-2009-2	Kd-2010-4	Kd-2011-1
SiO ₂	40.19	29.72	44.86	37.68
TiO ₂	1.51	1.33	2.12	1.55
Al ₂ O ₃	18.90	16.31	22.60	18.86
Fe ₂ O ₃ total Fe	22.18	8.00	5.35	16.62
MnO	0.21	1.64	0.15	<0.01
MgO	1.78	2.58	1.99	3.82
CaO	2.77	26.22	6.06	4.27
K ₂ O	3.64	2.04	4.81	2.09
P ₂ O ₅	<0.1	7.86	2.58	1.67
SO ₃ total S	8.67	3.16	9.32	13.29
NiO	0.10		0.16	
SrO	0.04	1.15		0.15
ZrO ₂				
Sum	100.00	100.00	100.00	100.00

The remaining constituents, itemized in Table 2, show varying amounts but with a concentration on Si, Al and Fe, subordinately on S. The Fe content, of magnetite or maghemite, possibly wuestite, is considered responsible for the magnetization of the chiemite (see Material).

4.2 SEM and microprobe analysis

A characteristic property of the porous (pore-sizes between 1 to 250 μm , Fig. 4) and almost pure glass-like black carbon matrix of the chiemite is the content of finely dispersed, light gray micrometer- and submicrometer-

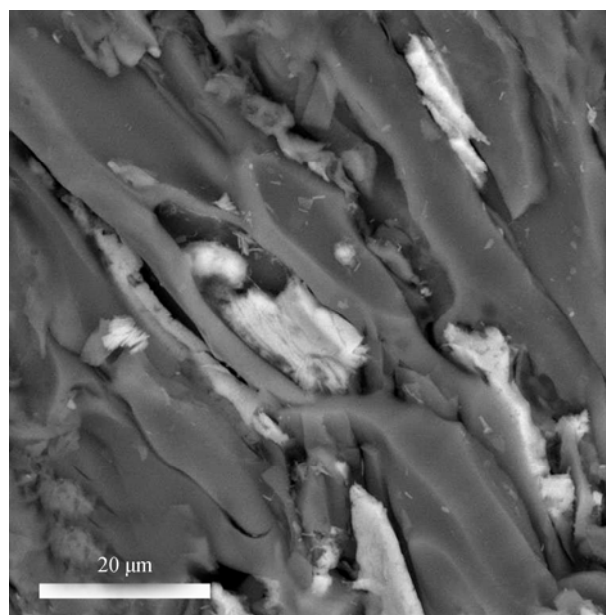


Fig. 5. SEM image of inclusions (light gray) within the carbon matter (dark gray) on the freshly crushed chiemite surface with relict fibrous texture of sample 2009-2.

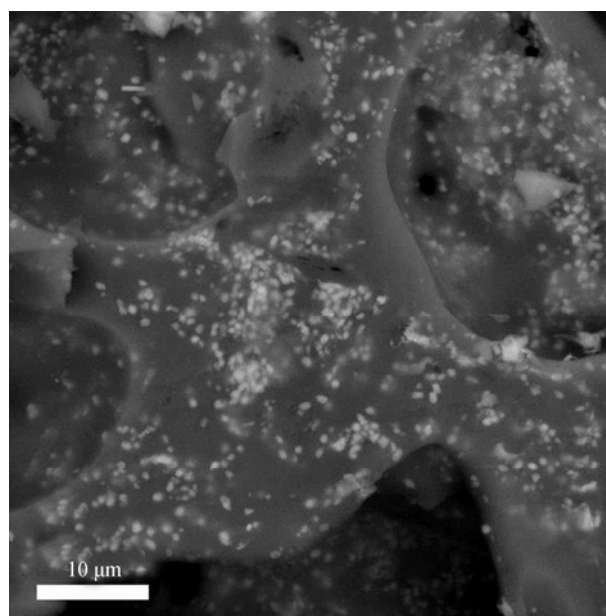


Fig. 6. SEM image of submicrometer-sized inclusions within the carbon matter of sample 2009-2.

sized inclusions, which have a complex composition of Ca, Cl, O, Mn, Cr, Fe, Na, K, Al, Si, and P (Figs. 5, 6, 7), where O, C, Al, Si (Fig. 7) originate from the chiemite carbon matrix. The analyzed mineral inclusions do not

match any known mineral composition. In addition, Figure 7 shows EDX spectra of the chiemite carbon matter and the complex chemical composition of the inclusions. Outstanding are the micrometer-sized Ag particles

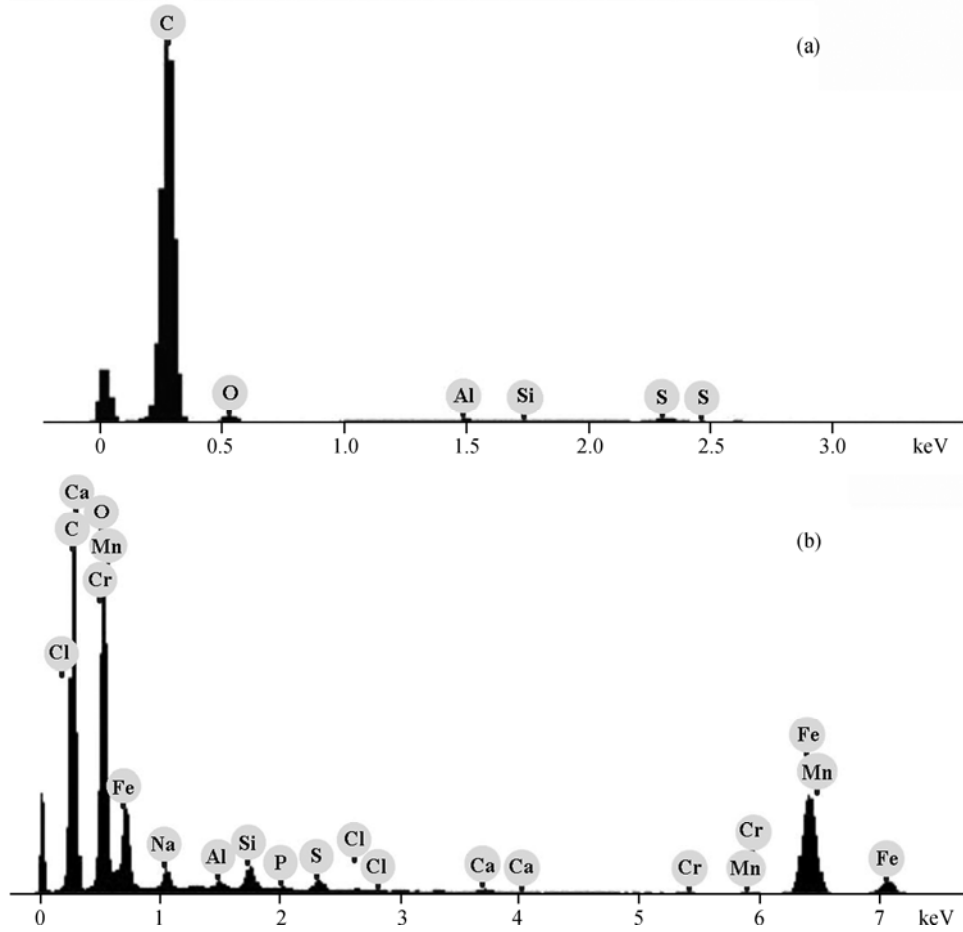


Fig. 7. EDX spectra.

(a), the chiemite carbon matter composition (corresponds to the grayish matter in Fig. 6); (b), light inclusions from Fig. 6 exhibiting a complex chemical composition. Specimen 2009-2.

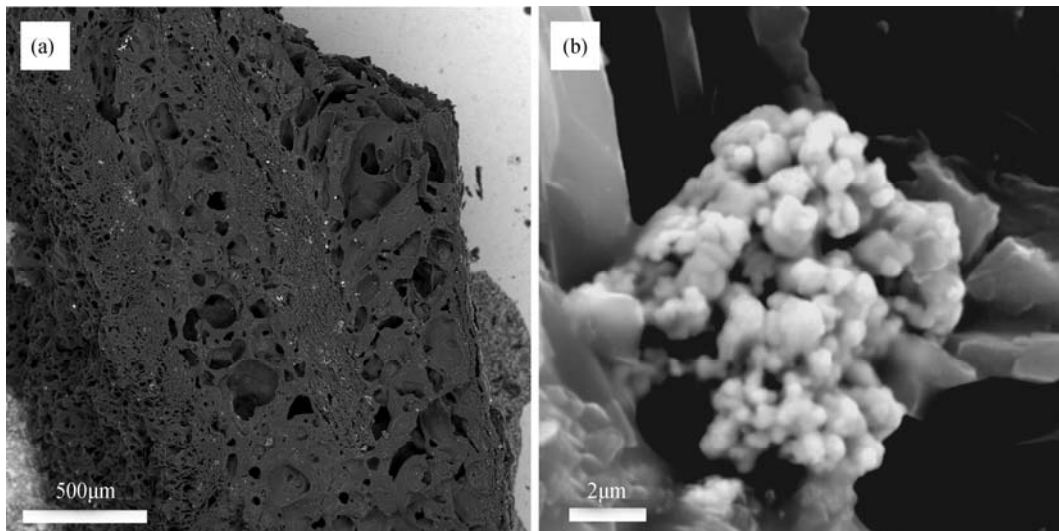


Fig. 8. (a), Distribution of white tiny silver inclusions within specimen 2009-2. (b), Ag aggregate (arrow in A) consisting of nanograins.

dispersed through the carbon matter, exhibiting as aggregates of small 200–600 nm grains (Fig. 8; EDX spectrum in Fig. 9).

4.3 X-ray diffraction

According to the X-ray diffraction studies, the analyzed chiemite carbon samples are characterized by wide peaks very similar to the parameters of glass-like carbon and shungite (Table 3, Fig. 10), whereas there is a large variation with regard to the full width at half of peak maximum (FWHM), which is known to depend on the sizes of the diffracting regions. For the studied chiemite samples the diffracting regions were essentially more varied in size than those in glass-like carbon and shungite. As a specific feature of the chiemite, we observe a quite sharp peak (FWHM=0.55–0.58 degree) corresponding to 2,083 Å, which can be attributed to (111) diamond reflection.

X-Ray synchrotron diffraction studies (Fig. 11) are in a good correspondence with the described above X-Ray data. However, following the synchrotron source investigations, we can estimate more evidently nanocrystalline graphite, diamond and the presence of some rock minerals sparsely dispersed within the chiemite. At the same time within a shungite sample just some quartz was measured, and as for glass-like carbon, no crystalline phases were found. From the general X-ray profile, the chiemite is characterized by wider peaks and correspondingly is in a more amorphous state in comparison to both shungite and glass-like carbon.

4.4 Atomic force microscopy; scanning spreading resistance microscopy

AFM data show various structures in different samples, from almost amorphous with rare globular inclusions (Fig. 12a, b) up to fully nano-globular structure (Fig. 12c, d). Except for sample 2009-2, and compared to glass-like carbon and shungite, the studied carbon chiemite structural elements (globules) have essentially smaller sizes (Fig. 12e, f; Table 4).

Electric properties were also studied in comparison with shungite. The data are presented by maps of electrical conductivity dispersion through an equal square (Fig. 13). For the electric regime only specimen 2009-2 was used because of the hillocky contact of the other specimens disabling cantilever study. According to Fig. 13, significantly different conductivity dispersion textures are evident, accentuating a very low density of conductive regions for the chiemite specimen in particular in comparison with the shungite matter at nanolevel (Figure 13). Thus, the chiemite is characterized by a massive nanostructure with rare highly conductive points whereas the shungite matter exhibits a layered nanostructure with essentially larger highly conductive regions. Here we refer to the observation that the difference between the nanostructure conductivity and the macroscopic chiemite electrical conductivity is considerable (see chapter "Material").

4.5 Transmission electron microscopy

Two specimens with essentially different ordering were studied with TEM where crystalline carbyne and diamond

Table 3 Powder X-ray diffraction data of carbon phases within chiemite samples in comparison with glass-like carbon and shungite

2 θ , degree	Peak height	Peak area	Full width at half maximum, degree	d (Å)	Δd (Å)	Diamond (hkl)	Graphite (hkl)
Kd-2006-1-1							
24,96	2348	428332	6,79	3,56	0,003		002
43,41	260	5014	0,55	2,083	0,001	111	
44,21	437	69537	5,28	2,057	0,001		101
79,98	138	35035	8,53	1,199	0,0002		110
Kd-2011-1							
25,21	2381	364618	5,51	3,539	0,03		002
43,37	138	2100	0,58	2,083	0,01	111	
44,11	386	47655	4,77	2,051	0,01		101
79,73	116	17620	4,96	1,202	0,003		110
Kd-2010-4							
24,63	1336	230317	7,38	3,61	0,01		002
26,68	385	2505	0,22	3,34	0,01		
44,01	186	29401	5,82	2,06	0,005		101
Kd-2009-2							
25,11	1196	247920	8,20	3,54	0,01		002
43,74	239	35737	5,80	2,07	0,005		101
80,64	86	6654	2,95	1,190	0,001		110
Shungite							
25,34	2662	393006	5,14	3,51	0,01		002
43,41	391	35437	2,80	2,08	0,005		101
78,91	95	14206	4,90	1,212	0,001		110
Glass-like carbon							
24,96	1940	342953	6,95	3,56	0,01		002
43,41	366	32555	3,41	2,08	0,005		101
79,63	122	17369	5,49	1,203	0,001		110

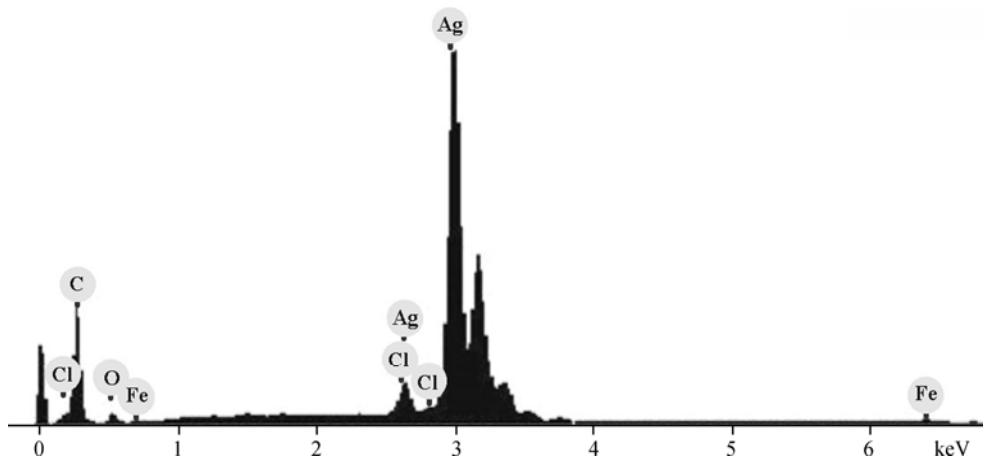


Fig. 9. EDX spectrum of a silver aggregate (corresponding to the Ag particle in Fig. 8b), C and O coming from the surrounding carbon matrix.

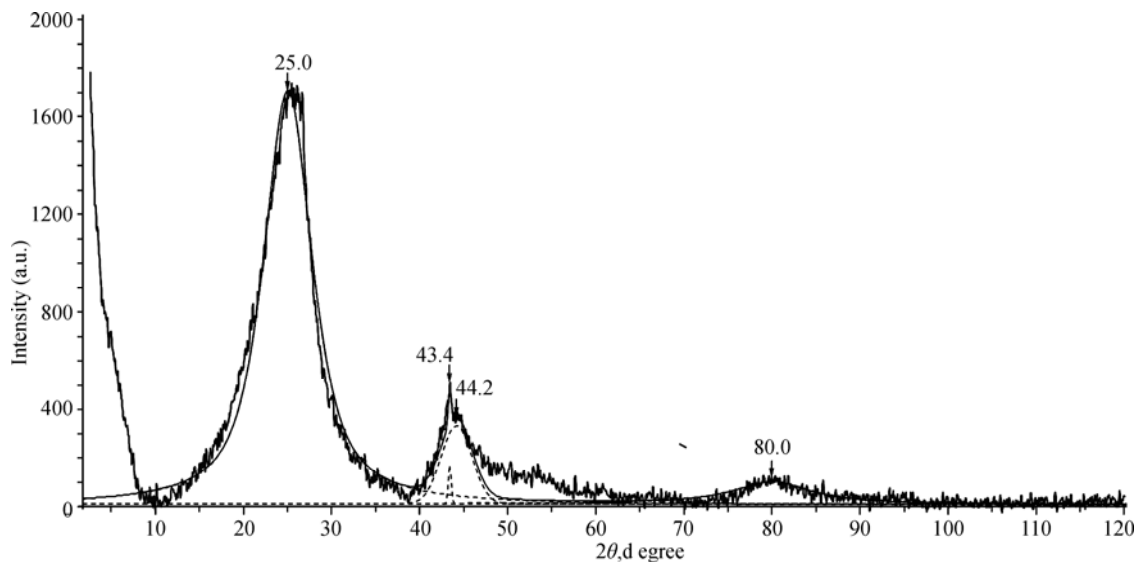


Fig. 10. Powder X-ray diffraction pattern of chiemite sample Kd-2006-1.

matter with different order levels have been analyzed: 1, Glass-like carbon—the glass-like carbon is the general carbon matter of chiemite, the structural features of which have been analyzed with TEM (Fig. 14) with good correspondence with X-ray diffraction and synchrotron X-ray diffraction; 2, Polycrystalline diamond, polynanocrystalline diamond, diamond-like carbon—in the course of Raman studies numerous optically transparent carbon particles have been found on the freshly crushed surfaces. The particles gained especial interest and were addressed by more deep studies using a combination of TEM and Raman analysis. Coordinates of the carbon particles with diamond structure identified by electron diffraction have been fixed within TEM grids and then studied by Raman spectroscopy in situ within TEM specimens on the same particles. Among the matter with the diamond nature of carbon we have found a whole suite of carbons, from quite good polycrystalline fine-grained aggregates, to polynanocrystalline diamond aggregates,

Table 4 Globule sizes according to AFM statistical data

Globule size, nm	Carbon samples				
	chiemite 2009-2	chiemite 2006-1	chiemite 2010-4	glass-like carbon	shungite
Average	50	18	17	30	39
Max	100	30	35	60	100
Entropy		8	8	9	9

and amorphous diamond-like carbon (Fig. 15). The fine-grained aggregates are exhibited in spot electron diffraction (SAED) patterns by thin rings with well-recognizable spots corresponding to reoriented diamond micrograins (Fig. 15a). Polynanocrystalline diamond aggregates are characterized by well-shaped rings without any spots due to their nanocrystalline structure (Fig. 15b). The diamond-like carbon is characterized by very wide faint rings belonging to amorphous diamond-like structure with corresponding absence of any crystalline structure (Fig. 15c).

4.6 Carbyne and graphite

The carbyne particles are characterized by different

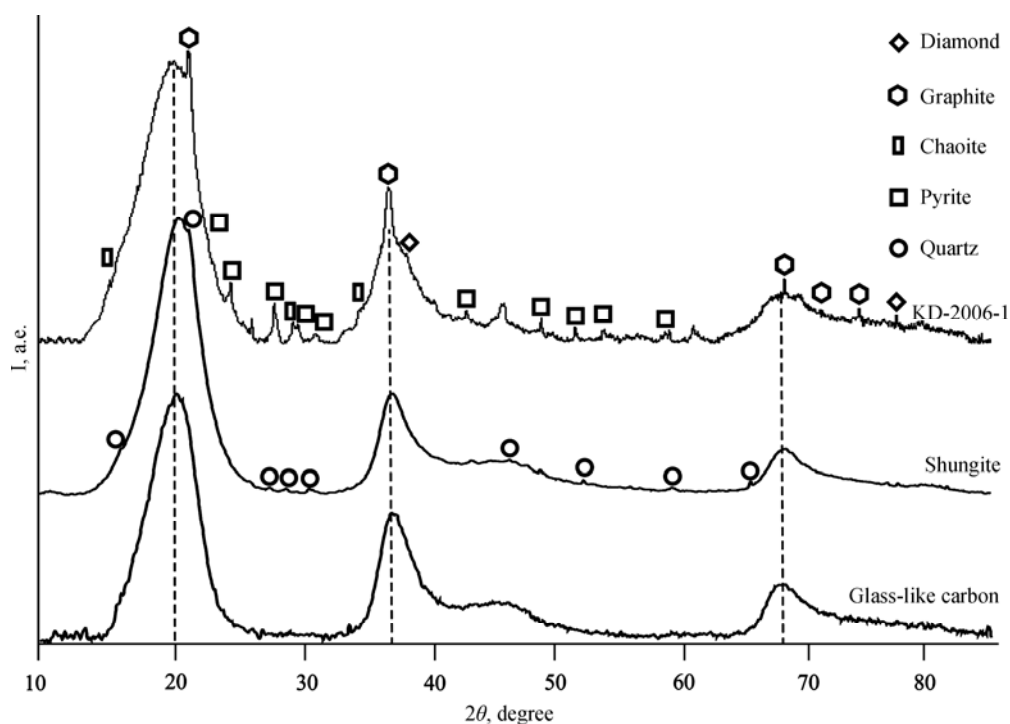


Fig. 11. X-Ray synchrotron diffraction patterns for chiemite (specimen KD-2006-1) in comparison with shungite (Shunga deposit, Russia) and glass-like carbon (SU-2000, Novocherkassk plant, Russia). Crystalline phases inclusions have been marked.

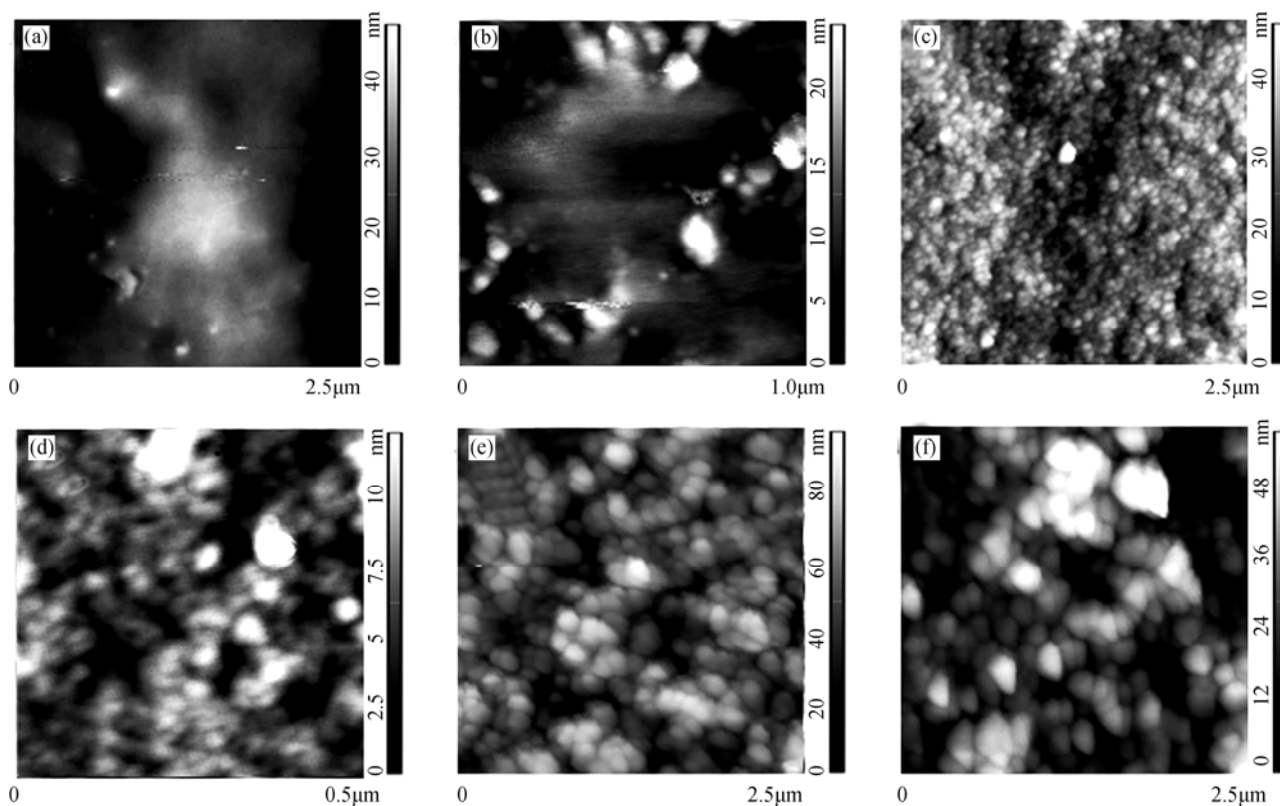


Fig. 12. AFM images.

(a, b), A freshly crushed surface displaying an almost amorphous structure, specimen 2009-2; (c, d), a freshly crushed surface displaying a globular structure, specimen 2010-4; (e, f), freshly crushed surfaces of shungite (e) and synthetic glass-like carbon (f) both displaying a globular structure. (e from Shun'ga deposit, Russia; f, glass-like carbon SU-2000 of Novocherkassk factory, Russia).

morphologies including irregular, flattened particles with pseudotriangular shape and nanosized globular elements easily recognized on bright field images (BF) (Fig. 16a, c). The two specimens both show well-ordered and absolutely amorphous matter, the different varieties being clearly seen in a selected area under SAED (Fig. 16b, d). According to

the SAED patterns, the crystalline variety for both specimens is represented by monocrystalline carbon (carbyne), principally the α -carbyne modification (Table 5). The β -carbyne was encountered in a spot diffraction pattern together with α -carbyne in coherently connected structure (Fig. 16d). It is interesting to note that the SAED

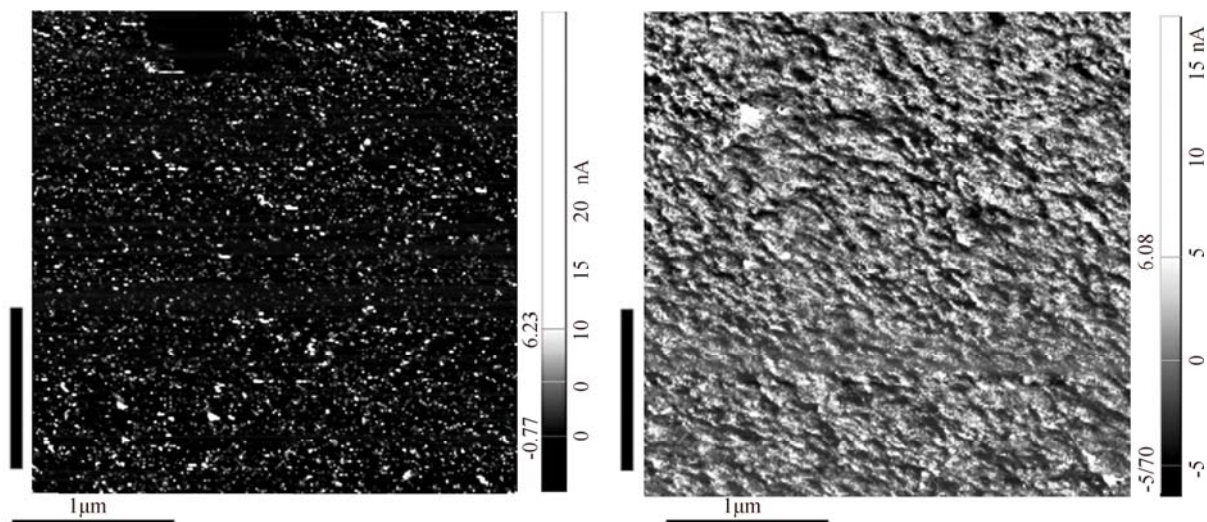


Fig. 13. SSRM images of electrical conductivity dispersion maps; chiemite (specimen 2009-2, left) and shungite (right). Shungite from Shun'ga deposit (Russia).

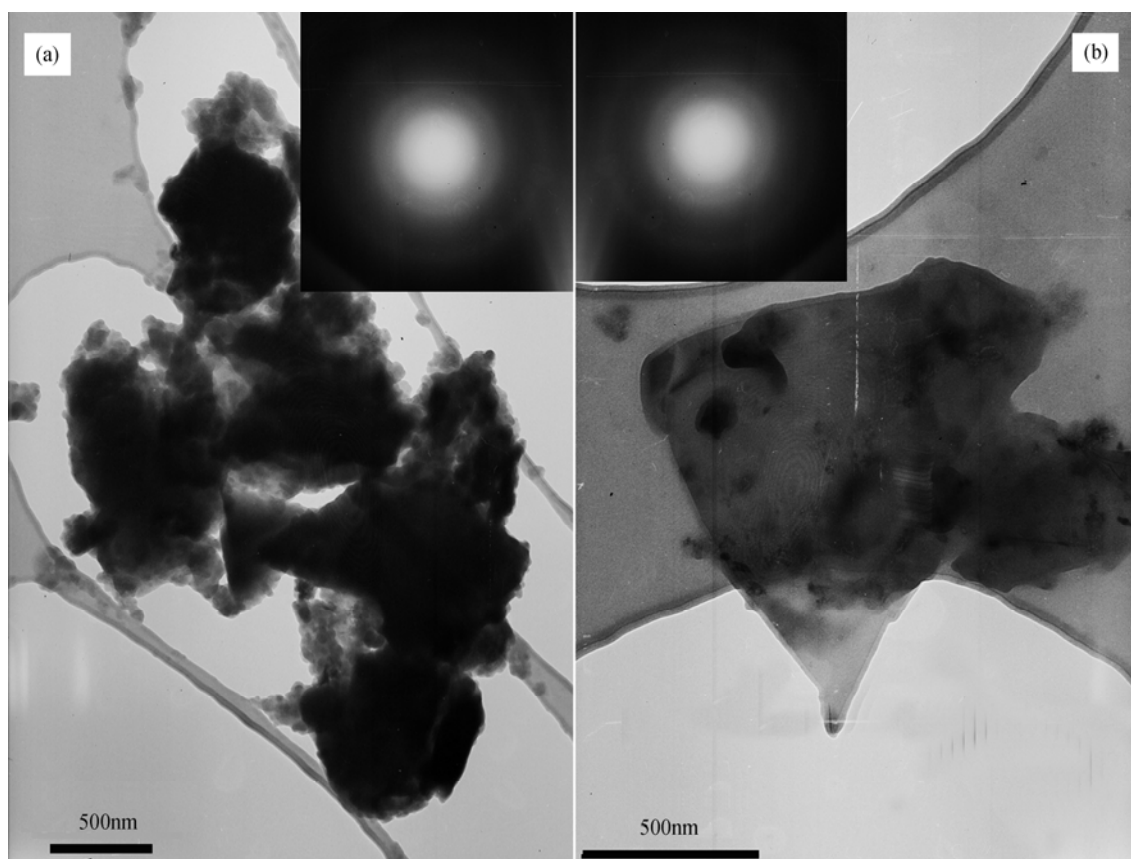


Fig. 14. BF (bright field) and corresponding SAED patterns of glass-like carbon pieces of the chiemite matrix. (a), specimen 2009-2; (b), specimen 2006-1.

study did not find any graphite particles among the crystalline material. However, attention should be drawn to the low stability of chiemite and carbyne under the electron beam as a special feature of the carbon matter, even at a very low energy (60 kV), which differs from synthetic glass-like carbon and natural shungite.

4.7 Raman spectroscopy: diamond carbons and carbyne

Raman spectroscopy (RS) analyses revealed the presence of submicrometer-sized, optically transparent carbon inclusions within the matrix (Fig. 17). To enable a correct identification, we extracted inclusion particles from crushed material that were then set on TEM grids to avoid mixing of Raman spectral signals of the inclusions and the host carbon matter. To avoid carbon film input into the spectra, the particles were laid upon carbon film holes. Under the optical microscope, the flattened irregular shapes of the inclusions became evident, but rare octahedron particles were also observed (Fig. 18). One of the most typical spectra of the optically transparent inclusions is presented in Fig. 19. The spectrum can be decomposed into three general wide bands: around 1325–1370, 1400–1500 and 1580–1600 cm^{-1} , and two bands on the down-shoulder side: around 1070–1090 and 1200–1250 cm^{-1} , and as such it does not match any spectrum of known carbon substances. On the other hand, the listed Raman features can be interpreted as amorphous carbon containing some quantity of amorphous diamond-like carbon (DLC), as we argue below.

The wide bands 1325–1370 and 1580–1600 cm^{-1} are

Table 5 Spot electron diffraction pattern data of α -carbyne from chiemite specimen 2006-1 in comparison with standard data (after Fedoseev et al., 1981)

Spot number	Specimen 2006-1			Standard data	hkl
	I, ball	d, nm	Δd , nm	d, nm	
1	8	0.443	0.004	0.447	110
2	10	0.255	0.002	0.257	300
3	8	0.221	0.002	0.223	220
4	6	0.168	0.001	0.169	410
5	8	0.148	0.0009	0.148	330
6	10	0.128	0.0007	0.129	600
7	4	0.123	0.0007	0.124	520
8	8	0.111	0.0007	0.112	440
9	Very weak	Not measured		0.102	170
10	2	0.097	0.0005	0.0976	630
11	6	0.088	0.0005	0.0895	550
12	8	0.087	0.0005	0.0861	900

expected to correspond to D and G Raman bands of carbon materials; Ferrari and Robertson (2004) stated that amorphous carbon with high content of tetrahedral carbon (ta-C) bonds has a low I_D/I_G relationship where increasing ta-C content involves decreasing I_D/I_G relationship. Additionally, it is required that the G band has to be downshifted. DLC shows a broad hump centered in the range 1510–1560 cm^{-1} and extending to 1300 cm^{-1} (Wei et al. 2000). Finally, full ta-C should have one very wide band around 1500 cm^{-1} (for 633 nm laser excitation) (Ferrari and Robertson 2004).

In our case the band at 1580–1600 cm^{-1} corresponds to the G carbon band featuring sp^2 carbon bonding within the matter. The band at 1325 cm^{-1} should be attributable to the D band of carbon substances, but the position is essentially downshifted from nominal about 1335 cm^{-1} for 633 nm excitation. This downshift can possibly be

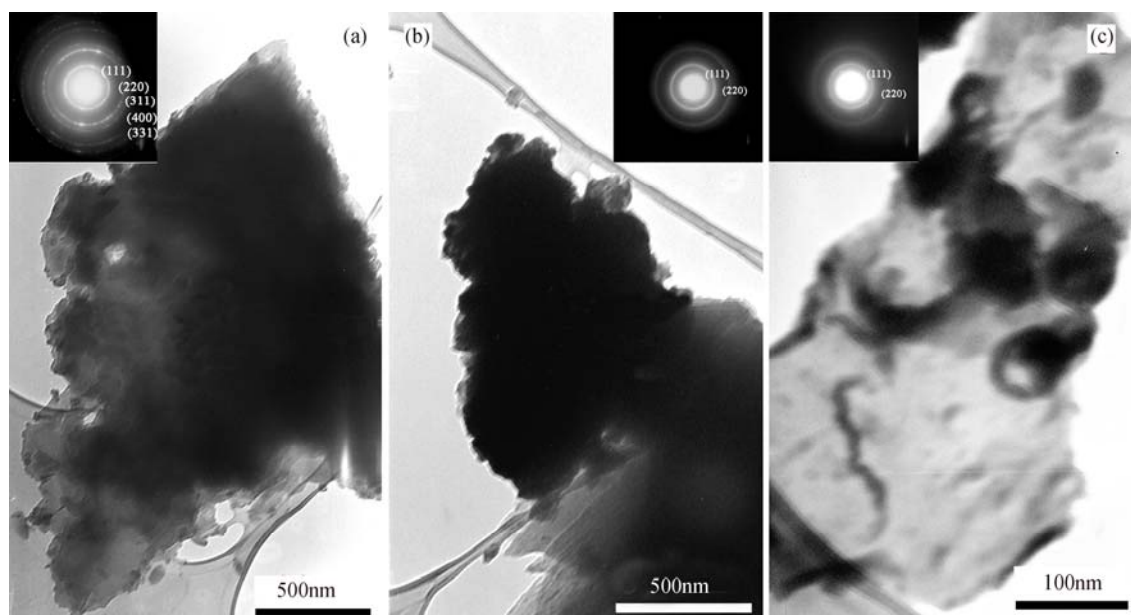


Fig. 15. BF and corresponding SAED patterns of carbon particles from the chiemite, specimen KD-2006-1. (a), polycrystalline diamond fine-grained aggregates; (b), polynanocrystalline diamond aggregates; (c), amorphous diamond-like carbon.

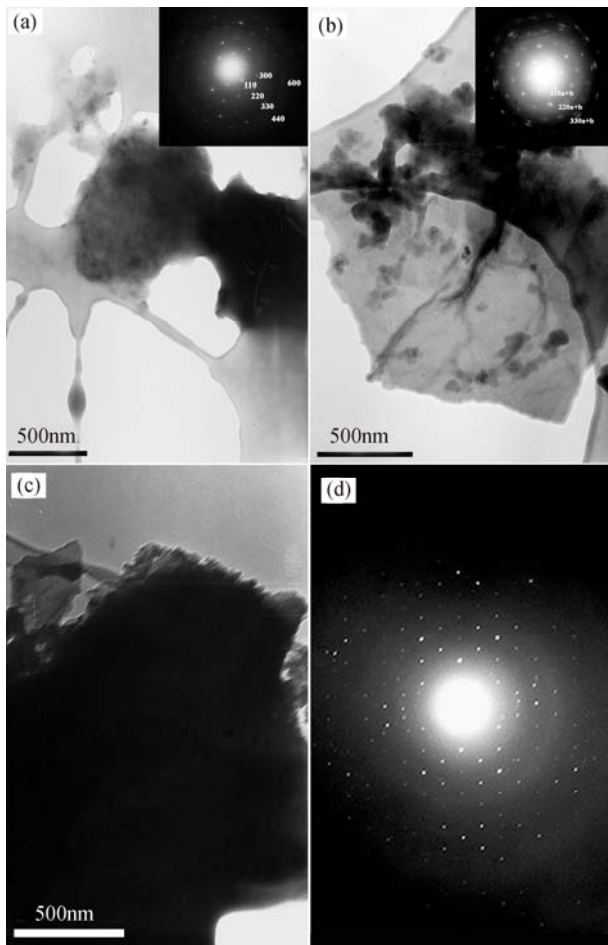


Fig. 16. BF and corresponding SAED patterns of carbyne particles.

(a), α -carbyne, specimen 2009-2; (b), co-oriented monocrystalline slightly textured α - and β -carbynes, $[001]\parallel$ beam, specimen 2006-1; (c), BF image of monocrystal of α -carbyne, specimen 2006-1; (d), SAED pattern from α -carbyne (corresponding to C image), $[001]\parallel$ beam, the corresponding interplanar distances are presented within Table 5.

ascribed to nanodiamond clusters (Filik et al. 2006) in agreement with the shape and optical properties of the particles, as shown in Fig. 20. The 1330 cm^{-1} band position as found for the optically nontransparent matter, however, is interpreted as the usual D band.

The peak $1070\text{--}1090\text{ cm}^{-1}$ corresponds well to the T peak, which comes from the vibrational density of the sp^3 states (Robertson 2002; Praver et al. 2000), or else to carbyne-like C=C bonds (Balzaretto et al. 2003). The deconvoluted, wide shoulder band at $1200\text{--}1250\text{ cm}^{-1}$ rather belongs to the phonon wave vectors from small vibrational domains and is quite usual in Raman spectra of nanodiamonds (Osswald et al. 2009; Praver et al. 2000). At the same time, it can be connected with the possible presence of carbyne-like carbon (Balzaretto et al. 2003).

The $\sim 1400\text{--}1500\text{ cm}^{-1}$ band can be observed with different intensity both in the optically transparent and the non-transparent carbon matter (Fig. 20). The band can be

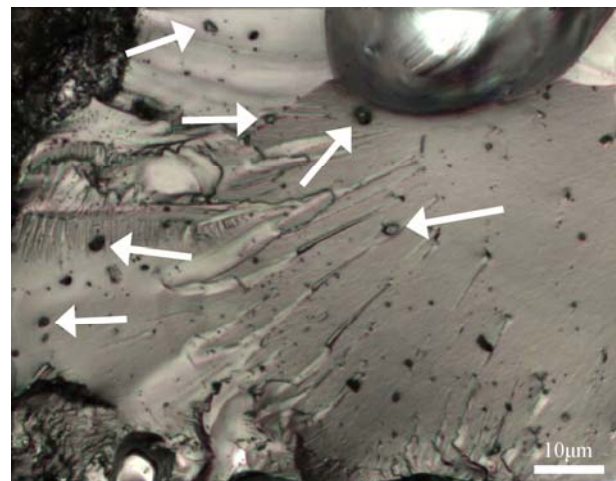


Fig. 17. Submicrometer-sized optically transparent carbon inclusions within the glass-like carbon matrix of the chiemite. Freshly crushed surface, reflected light. Specimen Kd-2006.

explained by transpolyacetylene C=C bonds, which can occur as independent nanoclusters or at nanograin boundaries (Balzaretto et al., 2003; Kavan and Kasher, 1999; Kudryavtsev et al., 1997; Ferrari and Robertson, 2001).

To summarize, we suggest that the analyzed optically transparent substance is possibly carbyne-like carbon or diamond-like carbon (Ding Xu-Li et al. 2009), whereas the nontransparent matter is rather amorphous graphite-like carbon with varying content of sp -carbon. This conclusion is supported by TEM data that demonstrate the presence of carbyne particles in a generally amorphous carbon matter. The structural details of coexisting sp^3 , sp^2 and sp carbons at nanolevel will be studied in future by electron energy loss spectroscopy mapping.

4.8 Fourier Transform Infrared (FTIR) Spectroscopy

The provided FTIR spectroscopy studies allowed us to recognize the high level of chiemite carbonization, which resulted from the very low content of C-H bonds (Fig. 21). The FTIR spectra are characterized by the low intensity of IR active bonds in a middle IR diapason exhibited by weak bands at 2850 and 2925 cm^{-1} , corresponding to C-H vibrations. The wide band at 1630 cm^{-1} can be attributed either to C=C or to C-O and C-H bonds; the very wide band centered at 1090 cm^{-1} should rather belong to C-C or/and C-O vibrations. The band at the spectral range $3100\text{--}1450\text{ cm}^{-1}$ (centered at 1450 cm^{-1}) results from absorbed water within the pressed specimen tabs. The FTIR spectra taken from different specimens demonstrate very similar data that underline the homogeneous structural features and heteroelements concentrations within chiemite matter.

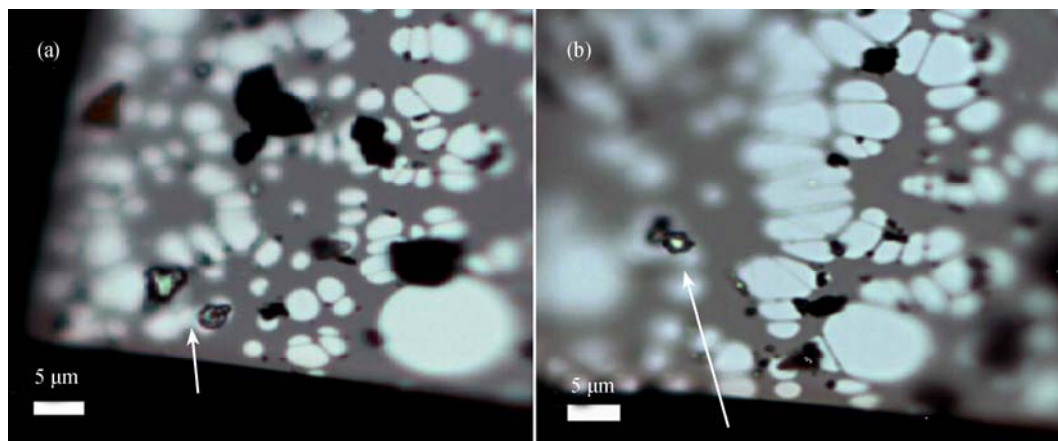


Fig. 18. Optically transparent diamonds (arrows); TEM grid specimens on a lacey carbon supporting film. (a), octahedron (specimen Kd-2009-2); (b), octahedron (specimen Kd-2006). Optical image, transparent light.

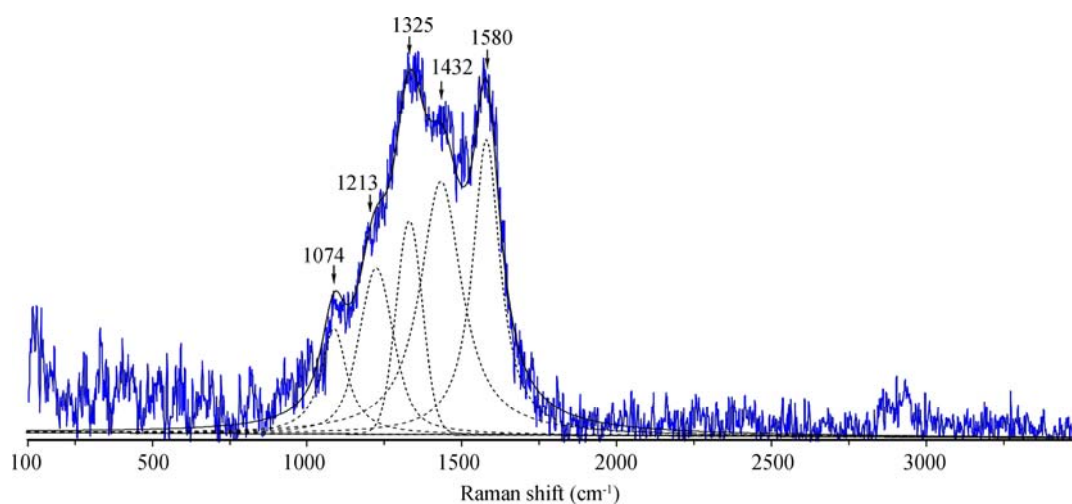


Fig. 19. Raman spectrum of amorphous diamond-like carbon of the particle from Figure 15b (specimen Kd-2006).

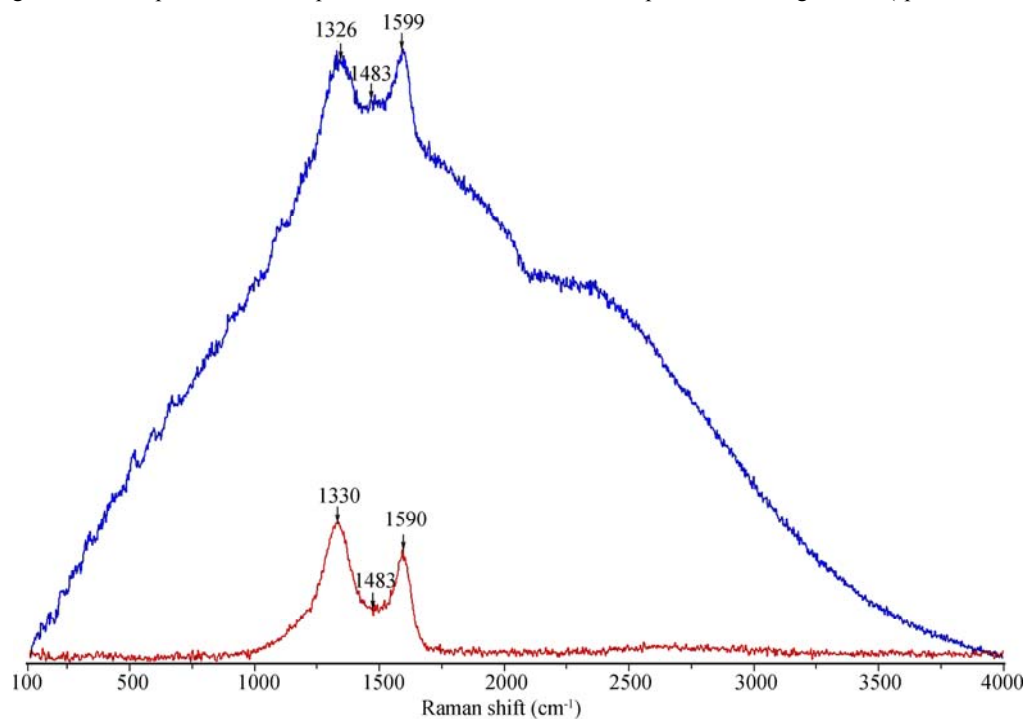


Fig. 20. Comparison of Raman spectra of optically transparent amorphous diamond-like carbon (upper spectrum) and optically nontransparent black glass carbon (bottom) (both figures specimen Kd-2006).

4.9 Differential thermal analysis (DTA)

According to DTA analysis, the chiemite carbon particles are different from sample to sample (Table 6). The thermal data are essentially higher than those for coal kerogen and closer to shungite and glass-like carbon; some parameters are even higher than all carbon standard materials (see 2006-1; 2011-1, Table 6).

4.10 Carbon isotopic data

Carbon $\delta^{13}\text{C}_{\text{PDB}}$ data have been measured for six chiemite samples from various localities (Table 7). They do not differ significantly and show values between -22.6 and -24.6% , which is near to the value, for example, of C3 plants, peats and coals (Liu lian et al. 2016; DingYingzhong et al. 2018).

Carbon-14 (^{14}C) isotopic data have been measured for two chiemite samples at the radiocarbon dating lab. at the Institute of Geography RAS (Moscow, Russia), IGAN-4196. It is especially important to note that both samples

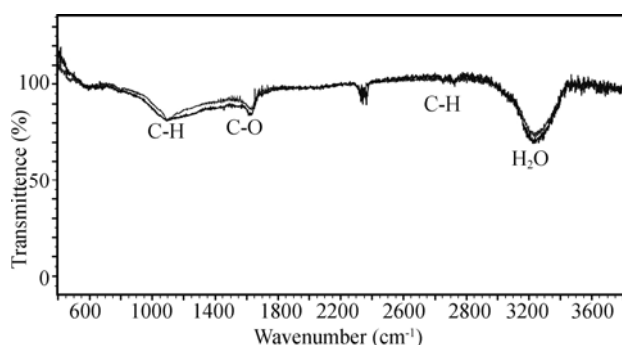


Fig. 21. FTIR spectra of chiemite from specimen 2006-1 (upper), and specimen 2011-1 (bottom). H_2O is a technological artifact, coming from specimen tabs pressed within water environment.

Table 6 DTA data for differently low ordered carbons and chiemite samples

Sample	Exothermal effect parameters ($^{\circ}\text{C}$)		
	Start temperature	Peak position	Final temperature
2009-2	268	413; 596	652
2010-4	383	612	784
2006-1	476	775	974
2011-1	511	737; 858	956
coal kerogen	187	307; 372; 424	582
shungite	433	628	802
glass-like carbon	495	697; 742	857
charcoal [*]	270-393	410-540	483-596

^{*}After Missio et al. (2014) and Zhuang et al. (2009).

Table 7 Delta ^{13}C data for chiemite samples

Sample, Lab. name	Full name	Isotopic data ($\%$)
		$\delta^{13}\text{C}_{\text{PDB}} \pm 1\sigma (= 0.15)$
Kd-2006-1	LID-RUH-2011-1	-24.4
Kd-2009-2	ROD-004U-2009-2	-22.6
Kd-2010-4	NEU-CHI-2010-4	-24.4
Kd-2011-1	ROT-CHI-2011-1	-24.2
Kd-NCH-2011	NEU-CHIE-2011-1,2	-23.6
Kd-LR-2011	LID-RUH-2011-1, 2, 3	-24.6

do not contain any concentrations of ^{14}C corresponding to an age of $> 48,000$ years BP. With regard to the superficial discovery position and the fresh sample shape this apparently early age is not easily understood and is addressed below.

5 Discussion

5.1 Basic properties

The chiemite carbon matter consists of different carbon phases. The matrix is a fully amorphous black glass-like carbon with a strongly porous structure and almost pure carbon content with traces of O, S, Si, Al and a few other elements. Inside the glassy carbon matter, diamond, amorphous diamond-like carbon and monocrystalline carbyne inclusions are found. During formation, an intense gas phase must have developed, which explains the strongly porous texture. Among the inclusions are native Ag particles present as fine-grained aggregates. According to Whittaker's phase diagram (e.g., Lamperti and Ossi 2003), carbyne is formed under a pressure of about 4–6 GPa and a temperature of 2,500–4,000 K. Graphite was found together with the carbyne as joint aggregates because of very high temperatures. Probable carbon glass is also within the chiemite, as seen from the RS, suggests temperatures as high as 3,800–4,000 K, following the carbon diagram. At these temperatures and with a fast decompression rate, solid phase formation (diamond, carbyne, carbon glass and some graphite) with possible partial sublimation into a gas phase could have occurred. The occurrence of a fossilized organic signature in the chiemite and relatively fresh wood particles encapsulated in the carbon matter show that organic matter was involved in the formation process. However, the obvious lack of ^{14}C must be explained either by an age exceeding c. 45,000 years or by isotope separation. In any case, the distribution of the chiemite excludes any long-term processes known from coal deposit formation and suggests the highest stages of coalification/carbonization in a young geologic environment. Although the matrix of the chiemite is porous and the morphology of the organic relicts has common features with biochars, described by Jindo et al. (2014), the other characteristics described above, i.e. thermal data (Table 6), the hardness, the diamond inclusions, diamond-like carbon allotropes and the carbyne, are essentially different. This points to a formation process far above the low-pressure coalification that occurs during biochar formation (Jindo et al. 2014). At the same time, and in addition, the preserved glass-like carbon chiemite after-wood pseudomorphs underscore the proximity to high-pressure carbon meteorite impact products such as the glass-like carbon and diamond,

recently described in the Kara astrobleme (Shumilova et al. 2018).

5.2 Formation

The chiemite carbon matter does not correspond to any known natural earth material with regard to the full array of data (Shumilova 2003). An industrial production whether intentionally or accidentally is totally unlikely. Carbyne and diamond formation are made under very special laboratory conditions (e.g., Chalifoux and Tykwinski 2010) and are incompatible with any known industrial processes known either in the study area or elsewhere. The wide distribution of occurrences in various environments is also incompatible with a formation happening purely by chance somewhere in an isolated industrial center hitherto completely unknown. The hypothetical reaction must have enabled wood particles to have survived within the extremely heated chiemite matrix (Fig. 3c). Moreover, the surprising lack of ^{14}C excludes an industrial origin from processing natural carbon material unless an unknown process was able to remove the radioactive isotope.

In nature, carbyne occurrences are known from a diamond mine in China (solely as flakes, Chuan et al. 2003), in Russia as single crystalline particles in graphite-bearing travertines (Shumilova et al. 2011; Danilova et al. 2016), and as carbyne chains within natural pseudomonocrystalline graphite from the Kumdykol deposit (Shumilova et al. 2018). Whittaker (1979) and Rietmeijer and Rotundi (2005) reported on natural carbynes on Earth (including chaoite), in meteorites, comets, circumstellar and interstellar dust, and also in natural graphite.

The relationship to organic material like wood may point to wildfires or forest fires from slash-and-burn land clearance practiced over millennia, but maximum temperatures of 800°C (in extreme cases 1200°C) are not enough by far as a source for chiemite origin, not to mention the pressures needed for carbyne and diamond formation. Moreover, the serious problem of the absence of ^{14}C remains as the observation that relatively fresh organic matter trapped within the chiemite could have survived the extreme heating. This latter feature points to procedures involving extreme temperatures and pressures in strongly non-linear processes such as those occurring in shock wave propagation in meteorite impact events, which resembles the chaoite occurrence in impactites from the Ries crater (El Goresy and Donnay 1968). Moreover, in recently published papers, impact glasses were shown to reveal encapsulated organic matter. In the Darwin glass, probably ejected from the 800-kyr old 1.2 km-diameter Darwin crater, Howard et al. (2013) established that

cellulose, lignin, aliphatic biopolymer and protein remnants did survive the impact. Glasses produced by Cenozoic meteorite impacts in Argentina were shown by Schultz et al. (2014) to reveal encapsulated plant matter in the form of macro-scale morphological biosignatures like vascular bundles, veins, phytoliths and papillae, as well as structures down to cellular level, and even evidence of organic matter. The authors describe the process of fossilization within the impact glass as instantaneous and as a snapshot of the target's ecology at the time of impact. Regarding the chiemite properties, the preserved wooden structures, the pseudomorphs after wood and the fresh wood particles encapsulated within the chiemite matrix, a formation process similar to the one that created the impact glass from Argentina is highly plausible.

Moreover, many characteristics of the chiemite (^{13}C isotopic composition, ordering level, carbons co-existence including the high-pressure carbon phases like diamond and diamond-like carbon, relict organics morphology, nanostructure) are rather similar to after-coal meteorite impact products (Shumilova et al. 2018; Ulyashev and Veligzhanin 2016) and can be described as a high-pressure carbon polymer, as reported by Yezerskiy (1982, 1986). The only essential differences are the high porosity and the presence of quite fresh wood fragments, which were preserved within the chiemite glass-like carbon matrix under high PT-conditions (Howard et al. 2013; Schultz et al. 2014).

Hence, we propose that the chiemite was formed by a meteorite impact shock that affected vegetation like wood, peat and coal from the impact target area, and that such an event clearly took place in the study region.

5.3 The Chiemgau impact event - probable source for chiemite formation

The Chiemgau strewn field dates to the Holocene Bronze Age/Celtic era (Schüssler et al. 2005; Rappenglück et al. 2009; Ernstson et al. 2010, 2012; Rappenglück et al. 2010; Liritzis et al. 2010; Hiltl et al. 2011), and comprises more than 80, mostly rimmed, craters scattered in a region about 60 km long by 30 km wide in the south-east of Germany (Fig. 1). The crater diameters range between a few to a few hundred meters. Geologically, the craters are embedded in Pleistocene moraine and fluvio-glacial sediments. The craters and surrounding areas feature heavy deformations of the Quaternary cobbles and boulders, and contain abundant fused rock material, such as impact melt rocks and various glasses, shock-metamorphic effects (planar deformation features [PDFs] in quartz, diaplectic glass from quartz and feldspar), geophysical (gravity, geomagnetic) anomalies (Ernstson et al. 2010; Neumair and Ernstson 2011) and widespread

impact-induced rock liquefaction features (Ernstson et al. 2011; Ernstson and Neumair 2011). Impact ejecta deposits in a catastrophic mixture contain polymictic breccias, shocked rocks, melt rocks, artifacts from Bronze Age/Celtic era people, charcoal and, as noted above, finely crushed wood fibers (Liritzis et al. 2010; Ernstson et al. 2010, 2013). The impact is substantiated by the abundant occurrence of metallic, glass and carbonaceous spherules, accretionary lapilli, microtektites (Ernstson et al. 2012, 2014) and of strange, possible meteoritic matter in the form of iron silicides like gupeite, xifengite, hapkeite, naquite and linzite, various carbides like, e.g., moissanite SiC and khamrabaevite (Ti, V, Fe) C, and calcium-aluminum-rich inclusions (CAI), minerals krotite and dicalcium dialuminate (Hiltl et al. 2011; Bauer et al. 2013; Rappenglück et al. 2013, 2014). Carbonaceous spherules contain fullerene-like structures and nanodiamonds that point to an impact-related origin (Yang et al. 2008). Such spherules were found embedded in the fusion crust of cobbles from one of the Chiemgau craters as well as in possible outfall found in soils over Europe (Rösler et al. 2005, 2006; Hoffmann et al. 2006; Yang et al. 2008). Physical (OSL) and, in the first place, archeological dating constrains the impact event to most probably between 2200 and 500 B.C. (Rappenglück et al. 2010; Liritzis et al. 2010). The impactor for the extensive strewn field is suggested to have been a roughly 1000-m sized low-density disintegrated, loosely bound asteroid or a disintegrated comet (Ernstson et al. 2010).

From the evidence of meteorite impact in the region of the chiemite finds, which is known to be related to extreme temperatures and pressures attaining more than 5,000 K and more than 100 GPa (see on impact cratering, e.g., French 1998; Melosh 1989), the basic properties of the chiemite gain a reasonable explanation. Apart from some Tertiary underground pitch coal beds in southern Bavaria, carbon from abundant carbonate rocks in the region can be discussed as a possible source for the chiemite origin. Hypervelocity impact experiments have confirmed the production of highly disordered graphite from dolomite or limestone targets (Bunch et al. 1997). For natural impacts, a transformation of CO to CO₂+C in the cooling atmospheric impact plume is assumed (Heymann and Dressler 1997). Miura et al. (1999a, b) proposed that amorphous carbon occurring in impact structures can be formed from vaporized limestone target rocks. Calcium contents within the carbon matter are interpreted to be remains from limestone target rocks. A carbonate source cannot be ruled out for the chiemite matter. Nevertheless, the isotopic $\delta^{13}\text{C}$ signature points toward an organic origin for its carbon content, which can be explained by the intimate relationship to the

macroscopic signature of vegetation, especially wood, observed within the glassy carbon of the chiemite. So, although a composite source for the chiemite remains viable, the presence of different material closely associated and affected by different P-T conditions within it, some being extreme (e.g. glassy carbon), is difficult to explain by a process other than a meteorite impact. Shock metamorphism of organic matter has so far been addressed only very slightly (e.g., Korochantsev et al. 2001), and, commonly, only the devastating visible effects upon vegetation, animals and humans exposed to meteorite impacts have been considered. In the last decades, organic matter (e.g., microorganisms) that has survived impact shock has increasingly become a matter of interest (Lindgren et al. 2006; Parnell and Lindgren 2006a, b; Parnell et al. 2005). Nevertheless, the reaction on the impact's target vegetation, that the very first 'layer' exposed to shock-wave propagation in the impact cratering process thereby underwent some kind of shock metamorphism, has never seriously been investigated. Of course, the vegetation covering the target area of larger impacts is, by volume, largely insignificant, and shock-produced carbon matter in older impact structures such as diamonds is always quickly ascribed, e.g., to graphite from metamorphic rocks. Hence, the widespread occurrence of the chiemite pieces with their exceptional properties in a very young impact area offers a good opportunity to better understand what could possibly happen to impact-shocked vegetation.

The hypothesis of impact-affected wood or other type of vegetation is further underlined when regarding the X-ray fluorescence analysis that reveals the composition of the chiemite non-carbon component (Table 2). These data have been compared (Fig. 22) with those from analyses for wood bottom ash from various sources in the USA and Canada (Naik et al. 2001). In both cases the scattering of individual values is considerable but on average and, except for SO₃, the percentage correspondence is remarkable, strongly supporting the impact hypothesis of chiemite formation by a meteorite impact. Also, the chiemite Carbon $\delta^{13}\text{C}_{\text{PDB}}$ data (Table 7) is near the values for C₃ plants and are also compatible with this hypothesis.

Proceeding from the concept model of a vegetation shock metamorphism, a basic drawback to be faced is that there is only vague knowledge of what really happened in the Chiemgau impact event. Commonly, in impact cratering studies, the contact and compression, excavation, and modification stages with the propagation of shock and rarefaction waves forming an impact crater are considered, and related shock pressures and temperatures affecting the underground rock materials are fairly well known (e.g., Melosh 1989; French 1998). Temperatures from shock

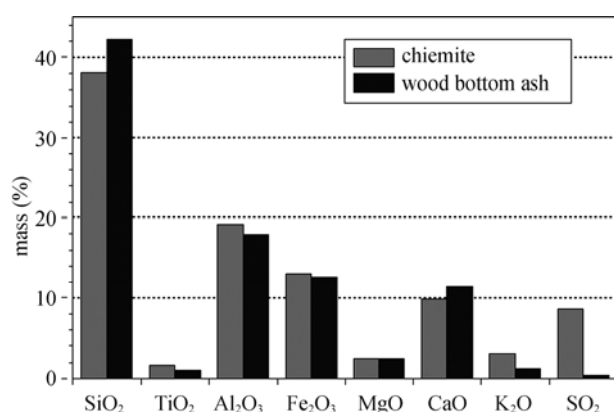


Fig. 22. X-ray fluorescence data (some major elements) of the chiemite (average values from Table 2) and wood bottom ash (average values from various sources in USA and Canada) (Naik et al. 2001); data for NiO, P₂O₅ and MnO (Tab. 2) not listed in Table 2 published by Naik et al. (2001). The chiemite data are the average from 4 specimens - Kd-2006-1, Kd-2009-2, Kd-2010-4 and Kd-2011-1, see Table 2).

release can attain several thousand degrees leading to complete vaporization and melting of rocks. The shock Hugoniot data for various wood species have been determined (Marsh 1980), and they are placed between liquids (e.g., water, Gojani, and Takayama 2008) and rocks. Hence, depending on impact velocities and shock pressures, wood can experience shock temperatures initiating ignition (about 300 °C) and in the extreme case temperatures enough for melting (about 4,000 K, valid for graphite, amorphous C) and vaporization (about 4,300 K, valid for graphite) of residual carbon. In addition, very high temperatures occur in large airbursts when weak cosmic bodies break up prior to impact, when much of the kinetic energy is transferred to the atmosphere, thus heating it (Wasson 2003). The temperatures are enough to melt the ground, as happens in nuclear explosion tests, as with the trinitite glass formation in the well-known Trinity event (Hermes and Strickfaden 2005). A similar process has been proposed for the origin of Libyan desert glass, for which the combined occurrence of a large airburst and impact of solid fragments has been demonstrated (Wasson 2003). Recent computer simulations (Boslough and Crawford, 2008) suggest that an exploding projectile moves downwards in the form of a high-temperature jet of expanding gas where temperatures can attain more than 5,000 K at the Earth's surface.

These general features may also apply to the Chiemgau impact event where crater diameters of up to several hundred meters are considered to have been formed by the impact of solid bodies. There is also much evidence of widespread effects of extreme heating of the ground combined with a probable formation of smaller craters not by impact but as pure explosion craters. This is concluded

from the occurrence of wide halos of intense rock melting and glass formation around the smaller rimmed craters (Rössler et al. 2006; Hoffman et al. 2005) that could not have resulted from the shock-release temperatures caused by a very small, meter-sized impactor (Ernstson et al. 2010). Moreover, anomalous distinct magnetic susceptibility peaks measured over large areas at some depth in the soil, for which an industrial or geogenic origin has been excluded (Hoffmann et al. 2004), could well be explained by an impact remagnetization due to the strong temperature overprint. Additionally, Neumair and Ernstson (2011) investigated unusually strongly magnetized limestone cobbles and boulders from some of the smaller craters, and Procházka and Kletetschka (2016) recently established that these limestone cobbles contain superparamagnetic magnetite or maghemite nanoparticles as the result of short-term high *PT* conditions. Hence, one or several airbursts in the Chiemgau area could well explain these observations, in particular regarding the low-density disintegrated, loosely bound asteroid or disintegrated comet proposed for the Chiemgau impact event (see above).

Keeping this in mind, the chiemite formation in the Chiemgau impact event attains some credibility, and a scenario of likely events can be outlined. Around 2200–500 BC, an incoming projectile turning into airbursts and heavy local explosions possibly from cometary gaseous components, together with solid fragments of the impactor must have impacted a densely forested landscape that also hosted large areas of bogs and peat deposits; this giant reservoir of organic matter exposed to impact shock and heat could have been the source for chiemite formation. Whereas, for the time being, it is largely unresolved as to what happened in detail, in particular regarding the role of shock pressure and temperature, probably most part of the vegetation simply burned. However, following a computer airburst simulation by Boslough and Crawford (2008), the most pertinent damage the vegetation underwent could have been high-temperature gas jets impinging on the ground, so that the characteristic chiemite texture with the strongly vesicular, pumice-like interior and flow structures (Figs. 4, 2c) can best be explained by rapid cooling from a degassing carbon melt where temperatures were high enough to produce the carbyne and diamond carbon allotropes. The additional role of shock pressure contribution to the chiemite formation must largely remain open, although the occurrence of highly shocked minerals (PDFs in quartz, diaplectic glass from feldspar maskelynite and quartz) in the impact area (see above) shows that impact pressures of more than 10 GPa were effective (e.g., Stöffler and Langenhorst 1994).

As a whole, the chiemite relationship to common rock

impactites becomes evident. Impact melt rocks are characterized by clastic debris in a crystalline or glass-like matrix that has solidified from shock-produced impact melt, and often reveal a vesicular and breccia-like texture. Likewise, the chiemite is composed of a glass-like (carbon) matrix that contains variable amounts of debris in the form of inclusions that clearly originate from finely dissected wood. These fragments that in fresh shape contribute to the catastrophic impact ejecta layers (see above) appear to have undergone some kind of fossilization similar to, but in fact unlike, charcoal because it resists burning. Comparable to the breccia-like texture of impact melt rocks, the chiemite can also be found as breccia-like fragments (Fig. 3d). Given the whole context, the at-first surprising, relatively fresh wood particles trapped within the chiemite matrix (Fig. 3c) may also be easily understood by taking a look at known impact cratering where rock fragments of drastically differing shock levels, from non-shocked to heavily shocked, can coexist in a single rock sample, and ejecta from stratigraphically quite distant layers can be found exposed on a decimeter scale. Here as a counterpart to the chiemite, we also reminded of the organic matter found encapsulated in the glass particles from the Darwin crater and Argentinian impacts and others mentioned above (Howard et al. 2013; Schultz et al. 2014).

Still unresolved is the process of the fossilization of the wood particles that attain a charcoal-like but non-flammable consistency. A possible explanation is that a strong impact shock could have been able to cause complete instantaneous evaporation and loss of volatile matter and water but in part preserve the original cellular structure. Also unresolved is how the chiemite could have formed pseudomorphs after wood fragments that frequently exhibit typical shapes of tree branches and bark. Here, a relationship to phytofulgurites is proposed; this new type of fulgurites that originate from a lightning strike on a haystack with resulting anthraxolite-like matter pseudomorphic after grass stems (Lysyuk et al. 2006), appears to be an interesting point for further study, in particular with regard to similar *PT* conditions during lightning strikes and meteorite impact. Furthermore, unresolved is the origin of nano-sized grains of Ag observed in the chiemite. The possible addition of silver from impact-affected prehistoric artifacts must remain speculative.

There remains the absence of any measurable radiocarbon content in the chiemite, because the geological setting excludes its formation from organic matter younger than 45,000 years. A possible industrial or major World War weapons action to the biomass can likewise be excluded. At the same time, we cannot

exclude an isotopic fractionation process for the ^{14}C , presumably caused by the impact event.

6 Conclusions

The unusual composition of the chiemite matter carrying diamond and carbyne allotropes suggests very high pressures and temperatures of formation, which we suggest formed in a natural process. The observations of this peculiar carbonization/coalification process cannot reasonably be ascribed to industrial or any other anthropogenic activities related to processes involving very high temperatures and pressures. Natural carbonization processes like wildfires cannot explain the manifold findings observed and analyses made. The high-*PT* carbon allotropes in direct contact with organic matter suggest a formation by the shock from a meteorite impact, and the intriguing conditions speak in favor of an immediate shock transformation from organic matter to high-rank carbon.

It is reasonable to explain the chiemite formation by meteorite impact shock with probable relationship to the Chiemgau meteorite impact, proposed as a large crater strewn field created only a few thousand years ago, which shows evidence of extreme pressures (shock effects like PDFs and diaplectic glass) and extreme temperatures (impact melt rocks, various impact glasses, microtektites) as well as typical meteorite-impact geological and geophysical features.

Such an impact origin for the chiemite formation is well supported by other comparable features generated after coal high-pressure carbon polymers containing different carbon phases, including diamond, diamond-like carbon, graphite and carbynes (Shumilova et al. 2018; Ulyashev and Veligzhanin 2016) along with preserved wood relict micromorphology.

The full details of the chiemite formation process remain unclear for now. The rich vegetation with extended forests and bogs in the impact target area are suggested as the principal elements for carbonization/coalification. A meteoritic carbon contribution of the impactor, an assumed comet or low-density "rubble pile" asteroid, cannot be excluded.

Altogether, field observations of the chiemite occurrence is so far restricted to the meteorite impact strewn field, and laboratory analyses are consistent with chiemite formation in an impact event. This supports the idea of a new type of a (carbon) impactite that might possibly exist elsewhere in a similar situation and may also be observed with other, younger and older impacts.

With regard to recently increased discussions on organic matter in impact structures and the extreme

conditions in which organisms can survive impact, which is considered important for astrobiology, the chiemite occurrences and properties may contribute to the topic. Finally, the present results seem to underline the prediction of Shumilova et al. (2018) for a more widespread occurrence of impact diamonds than has hitherto been accepted. Diamond- and carbyne-bearing chiemite can be produced from fresh wood and peat via meteorite impact carbonization, adding a novel source of carbon to the formation of the different impact-induced carbon allotropes.

Acknowledgements

This study was supported for the Russian team members by the RFBR, Project # 17-05-00516. The authors would like to thank the group of local amateur researchers and archeologists for their tireless efforts in the field work and the sampling of chiemite specimens. We would also like to thank M.A. Samotolkova, S.S. Shevchuk, V.A. Radaev, I.V. Smoleva, E.P. Zazovskaya for their help in analytical studies, and Dr. V. Kvasnytsya, Dr. S. Genest, Dr. S. Turner and an anonymous reviewer for meticulous reviews and language improvements.

Manuscript received Mar. 8, 2018

accepted Jun. 21, 2018

edited by Susan Turner and Fei Hongcai

References

- Balzaretti, N.M., Perottoni, C.A., and Jornada, J.A.H., 2003. High-pressure Raman and infrared spectroscopy of polyacetylene. *Journal of Raman Spectroscopy*, 34: 259–263
- Bauer, F., Hiltl, M., Rappenglück, M.A., Neumair, A., and Ernstson, K., 2013. Fe₂Si (Hapkeite) from the subsoil in the alpine foreland (Southeast Germany): is it associated with an impact? 76th Annual Meteoritical Society Meeting. *Meteoritics & Planetary Science*, 48(s1), Abstract #5056.
- Boslough, M.B.E., and Crawford, D.A., 2008. Low-altitude airbursts and the impact threat. *Int. J. Impact Engineering*, 35 (12): 1441–1448.
- Bunch, T.E., Becker, L., Schultz, P.H., and Wolbach, W.S., 1997. New potential sources for Black Onaping carbon. In: *Conferences on Large Meteorite Impacts and Planetary Evolution* (Sudbury 97), p. 7, LPI Contributions No. 922, Lunar and Planetary Institute, Houston.
- Castelli, I.E., Salvestrini, P., and Manini, N., 2012. Mechanical properties of carbynes investigated by ab initio total-energy calculations. *Physical Review B*, 85(21): 214110.
- Chalifoux, W.A., and Tykwinski, R.R., 2010. Synthesis of polyynes to model the sp-carbon allotrope carbyne. *Nature Chemistry*, 2: 967–971.
- Chernyshov, A.A., Veligzhanin, A.A., and Zubavichus, Y.V., 2009. Structural Materials Science end-station at the Kurchatov Synchrotron Radiation Source: Recent instrumentation upgrades and experimental results // Nucl. Instruments Methods Phys. Res. Sect. A Accel. Spectrometers, Detect. Assoc. Equip. 603: 95–98.
- Chuan, X.Y., Zheng, Z., and Chen, J., 2003. Flakes of natural carbyne in a diamond mine. *Carbon*, 41(10): 1877–1880.
- Correa, A.A., Bonev, S.A., and Galli, G., 2006. Carbon under extreme conditions: phase boundaries and electronic properties from first-principles theory. *PNAS*, 103 (5): 1204–1208.
- Courbion, G., and Ferey, G., 1988. Na₂Ca₃Al₂F₁₄: A new example of a structure with “independent F³⁻”—A new method of comparison between fluorides and oxides of different formula // *J. Solid State Chem.*, 76: 426–431.
- Danilova, YuV., Shumilova, T.G., Mayer, J., and Danilov, B.S., 2016. Conditions and formation mechanism of carbon phases in Late Quaternary geyzerites and travertines of Ol’khon area and Ol’khon Island (Baikal Rift Zone). *Petrology*, 24(1): 35–48.
- Ding Xu-Li, Li Qing-Shan and Kong Xiang-He, 2009. Optical and electrical properties evolution of diamond-like carbon thin films with deposition temperature. *Chinese Physical Letters*, 26(2): 027802.
- El Goresy, A., and Donnay, G., 1968. A new allotropic form of carbon from the Ries Crater. *Science*, 161: 363–364.
- El Goresy, A., Gillet, P., Chen, M., Kunstler, F., Graup, G., and Stähle, V., 2001. In situ discovery of shock-induced graphite-diamond transition in gneisses from the Ries crater, Germany. *American Mineralogist*, 86: 611–621.
- El Goresy, A., Dubovrinsky, L., Gillet, P., Mostefaoui, S., Graup, G., Drakopoulos, M., Simionovici, A.S., Swamy, V., and Masaitis, V.L., 2003. A novel cubic, transparent and super-hard polymorph of carbon from the Ries and Popigai craters: implications to understanding dynamic-induced natural high-pressure phase transitions in the carbon system. *34th Lunar and Planetary Science Conference*, 1016.pdf.
- Ernstson, K., Hilt, M., and Neumair, A., 2014. Microtektite-Like Glasses from the Northern Calcareous Alps (Southeast Germany): Evidence of Proximal Impact Ejecta. *45th Lunar and Planetary Science Conference*, 1200.pdf see above.
- Ernstson, K., Mayer, W., Neumair, A., Rappenglück, B., Rappenglück, M.A., Sudhaus, D., and Zeller, K.W., 2010. The Chiemgau crater strewn field: evidence of a Holocene large impact in southeast Bavaria, Germany. *J. Siberian Federal University, Engineering & Technology*, 1(3): 72–103.
- Ernstson, K., and Neumair, A., 2011. Geoelectric complex resistivity measurements of soil liquefaction features in Quaternary sediments of the Alpine Foreland, Germany. Fall Meeting, 5–9 Dec. 2011, *Abstracts. San Francisco: AGU*, NS23A-1555.
- Ernstson, K., Shumilova, T.G., Isaenko, S.I., Neumair, A., and Rappenglück, M.A., 2013. From biomass to glassy carbon and carbynes: evidence of possible meteorite impact shock coalification and carbonization. Modern problems of theoretical, experimental and applied mineralogy (Yushkin Memorial Seminar 2013). *Proceedings of mineralogical seminar, Syktyvkar*. IG Komi SC UB RAS: 369–371.
- Ernstson, K., Mayer, W., Neumair, A., and Sudhaus, D., 2011. The sinkhole enigma in the alpine foreland, Southeast Germany: Evidence of impact-induced rock liquefaction processes. *Centr. Eur. J. Geosci.* 3(4): 385–397.
- Ernstson, K., Sideris, C., Liritzis, I., and Neumair, A., 2012. The Chiemgau meteorite impact signature of the Stöttham

- archaeological site (southeast Germany). *Mediterranean Archaeology and Archaeometry*, 12: 249–259.
- Fedoseev, D.V., Novikov, N.V., and Teremetskaya, I.G., 1981. Diamond. In: Novikov, N.V. (ed.), *Diamond Reference book*. Kiev: Naukova Dumka, 77 (in Russian).
- Ferrari, A.C., and Robertson, J., 2001. Resonant Raman spectroscopy of disordered, amorphous, and diamondlike carbon. *Physical Review B*, 64: 075414.
- Ferrari, A.C., and Robertson, J., 2004. Raman spectroscopy of amorphous, nanostructured, diamond-like carbon, and nanodiamond. *Phil. Trans. Royal Soc. London, A*, 362: 2477–2512.
- Filik, J., Harvey, J.N., Allan, N.L., May, P.W., Dahl, J.E.P., Liu, S., and Carlson, R.M.K., 2006. Raman spectroscopy of nanocrystalline diamond: An *ab initio* approach. *Physical Review B*, 74, 035423.
- French, B.M., 1998. *Traces of Catastrophe: a Handbook of Shock-metamorphic Effects in Terrestrial Meteorite Impact Structures*. Houston, TX: Lunar and Planetary Institute, 120.
- Gojani, A.B., and Takayama, K., 2008. Experimental Determination of Shock Hugoniot for Water, Castor Oil, and Aqueous Solutions of Sodium Chloride, Sucrose and Gelatin. *Materials Science Forum*, 566: 23–28.
- Hammersley, A.P., 2016. FIT2D: a multi-purpose data reduction, analysis and visualization program. *J. Appl. Crystallogr.* 49: 646–652.
- Hermes, R., and Strickfaden, W., 2005. New theory on the formation of trinitite. *Nuclear Weapons Journal*, 2: 2–7.
- Heymann, D., and Dessler, B., 1997. Raman study of carbonaceous matter and anthroxolite in rocks from the Sudbury, Ontario, impact structure. 28th Lunar and Planetary Science Conference, 1268.pdf. see above.
- Hiltl, M., Bauer, F., Ernstson, K., Mayer, W., Neumair, A., and Rappenglück, M.A., 2011. SEM and TEM analyses of minerals xifengite, gupeite, Fe₂Si (hapkeite?), titanium carbide (TiC) and cubic moissanite (SiC) from the subsoil in the Alpine Foreland: Are they cosmochemical? 42nd Lunar and Planetary Science Conference, 1391.pdf see above.
- Hoffmann, V., Rösler, W., and Schibler, I., 2004. Anomalous magnetic signature of top soils in Burghausen area, SE Germany. *Geophys. Res. Abstr.* 6: 05041.
- Hoffmann, V., Rösler, W., Patzelt, A., Raeymaekers, B., and Van Espen, P., 2005. Characterisation of a small crater-like structure in SE Bavaria, Germany. *Meteor. Planet. Sci.* 40: A129.
- Hoffmann, V., Torii, M., and Funaki, M., 2006. Peculiar magnetic signature of Fe-silicide phases and diamond/fullerene containing carbon spherules. In: *10th Castle Meeting on New Trends in Geomagnetism*. Travaux Géophysiques XXVII (27): 52–53.
- Howard, K.T., Bailey, M.J., Berhanu, D., Bland, P.A., Cressey, G., Howard, L.E., Jeynes, C., Matthewman, R., Martins, Z., Sephton, M.A., Stolojan, V., and Verchovsky, S., 2013. Biomass preservation in impact melt ejecta. *Nature Geosci.* 6: 1018–1022.
- Isaenko, S., Shumilova, T., Ernstson, K., Shevchuk, S., Neumair, A., and Rappenglück, M., 2012. Carbynes and DLC in naturally occurring carbon matter from the Alpine Foreland, South-East Germany: Evidence of a probable new impactite. *Eur. Min. Conf.*, Vol. 1, EMC2012-217, 2012.
- Itoh, M., Kotani, M., Naito, H., Sunada, T., Kawazoe, Y., and Adschiri, T., 2009. New metallic carbon crystal. *Physics Rev. Lett.* 102 (5): 055703.
- Jindo, K., Mizumoto, H., Sawada, Y., Sanchez-Monedero, M.A., and Sonoki, T., 2014. Physical and chemical characterization of biochars derived from different agricultural residues. *Biogeosciences*, 11: 6613–6621.
- Kavan, L., and Kasher, J., 1999. Molecular and electron spectroscopy of carbyne structures. In: Heimann, R.B., Evsyukov, S.E., and Kavan, L. (eds.), *Carbyne and Carbynoid Structures*. Dordrecht: Kluwer, 343–356.
- Korochantsev, A.V., Badjukov, D.D., and Sadilenko, D.A., 2001. Shock metamorphism of organic matter. *Meteor. Planet. Sci.*, 36(9): A104
- Kudryavtsev, Yu. P., Evsyukov, S., Guseva, M., Babaev, V., and Khvostov, V., 1997. Carbyne – a linear chainlike carbon allotrope. In: Thrower, P.A. (ed.), *Chemistry and Physics of Carbon*. New York-Basel-Hong Kong: Marchel Dekker Inc., 2–70.
- Lamperti, A., and Ossi, P.M., 2003. Energetic condition for carbyne formation. *Chem. Phys. Lett.* 376: 662–665.
- Lin, Y., Zhang, L., Mao, H., Chow, P., Xiao, Y., Baldini, M., Shu, J., and Mao, W.L., 2011. Amorphous diamond: A high-pressure superhard carbon allotrope. *Phys. Rev. Lett.* 107: 175504.
- Lindgren, P., Parnell, J., Bowden, S.A., Taylor, C., Osinski, G.R., and Lee, P., 2006. Preservation of biological signature within impact melt breccias, Haughton Impact Structure. 37th Lunar and Planetary Science Conference, 1028.pdf
- Liritzis, I., Zacharias, N., Polymeris, G.G., Kitis, G., Ernstson, K., Sudhaus, D., Neumair, A., Mayer, W., Rappenglück, M.A., and Rappenglück, B., 2010. The Chiemgau meteorite impact and tsunami event (southeast Germany): first OSL dating. *Mediterranean Archaeology and Archaeometry*, 10(4): 17–33.
- Liu Lian, Huang Hin and Liu Zhiqiang, 2016. Stable carbon isotopic composition of black carbon in surface soil as a proxy for reconstructing vegetation on the northern slope of the Qinling Mountains. *Acta Geologica Sinica (English Edition)* 90(1): 222–229.
- Liu, M., Artyukhov, VI, Lee, H., Xu, F., and Yakobson, B.I., 2013. Carbyne from first principles: chain of C atoms, a nanorod or a nanorope. *ACS Nano*, 7(11): 10075–10082.
- Lysyuk, AYU, Yurgenson, G.A., and Yushkin, N.P., 2006. Phytofulgurites: A new type of geological formations. *Doklady Earth Sciences*, 411: 1431–1434.
- Marsh, S.P. (ed.), 1980. *LASL Shock Hugoniot Data*. Berkeley, Los Angeles and London: University of California Press, 658.
- Masaitis, V.L., Futergendler, S.I., and Gnevushev, M.A., 1972. Diamonds in impactites of the Popigai meteoritic crater. *Zapiski Vsesoyuznogo Mineralogicheskogo Obshestva*, 101 (1): 108–112 (in Russian).
- Melosh, H.J., 1989. *Impact cratering: A geologic process*. New York: Oxford University Press.
- Missio, A.L., Mattos, B.D., Gatto, A.A., and de Lima, E.A., 2014. Thermal analysis of charcoal from fast-growing eucalypt wood: influence of raw material moisture content. *J. Wood Chemistry and Technology*, 34: 191–201.
- Miura, Y., Fukuyama, S., and Gucsik, A., 1999a. Compositional changes by multiple impacts. *J. Materials Processing Technology*, 85: 192–193.
- Miura, Y., Kobayashi, H., Kedves, M., and Gucsik, A., 1999b.

- Carbon source from limestone target by impact reaction at the K/T boundary. *30th Lunar and Planetary Science Conference*, 1522–1523.
- Naik, T.R., Kraus, R.N., and Kumar, R., 2001. *Wood Ash: A New Source of Pozzolan Material*. - Report No. CBU-2001-10 REP-435, Department of Civil Engineering and Mechanics, College of Engineering and Applied Science, The University of Wisconsin, Milwaukee.
- Narayan, J., and Bhaumik, A., 2015. Novel phase of carbon, ferromagnetism, and conversion into diamond. *J. Appl. Phys.*, 118: 215303.
- Neumair, A., and Ernstson, K., 2011. *Geomagnetic and morphological signature of small crateriform structures in the Alpine Foreland, Southeast Germany*. Fall Meeting, 5-9 Dec. 2011, Abstracts. San Francisco: AGU, GP11A-1023. usual citation
- Osswald, S., Mochalin, V.N., Havel, M., Yushin, G., and Gogotsi, Y., 2009. Phonon confinement effects in the Raman spectrum of nanodiamond. *Physical Review B*, 80, 075419.
- Pan, B., Xiao, J., Li, J., Liu, P., Wang, C., and Yan, G., 2015. Carbyne with finite length: The one-dimensional sp carbon. *Science Advances*, 1(9) me1500857.
- Parnell, J., Lee, P., Osinski, G.R., and Cockell, C.S., 2005. Application of organic geochemistry to detect signatures of organic matter in the Haughton impact structure. *Meteor. Planet. Sci.* 40: 1879–1885.
- Parnell, J., and Lindgren, P., 2006a. The processing of organic matter in impact craters: implications for the exploration of life. In: *Proceedings of the First International Conference on Impact Cratering in the Solar System*. ESLAB430-Proc_288838-Parnell.pdf, 147–152, European Space Agency.
- Parnell, J., and Lindgren, P., 2006b. Survival of reactive carbon through meteorite impact melting. *Geology*, 34: 1029–1032.
- Praver, S., Nugent, K.W., Jamieson, D.N., Orwa, J.O., Bursill, L.A., and Peng, J.L., 2000. The Raman spectrum of nanocrystalline diamond. *Chem. Phys. Lett.* 332: 93–97
- Procházka, V., and Kletetschka, G., 2016. Evidence for superparamagnetic nanoparticles in limestones from Chiemgau crater field, SE Germany. 47th Lunar and Planetary Science Conference, 2763.pdf see above.
- Rappenglück, B., Ernstson, K., Mayer, W., Neumair, A., Rappenglück, M.A., Sudhaus, D., and Zeller, K.W., 2009. The Chiemgau impact: An extraordinary case study for the question of Holocene meteorite impacts and their cultural implications. In: Belmonte, J. A. (ed.), *Proceedings of the International Conference on Archaeoastronomy, SEAC 16th 2008 "Cosmology across Cultures*. Impact of the Study of the Universe in Human Thinking", Granada September 8-12, 2008, A.S.P. Conf. Ser., 2009.
- Rappenglück, B., Rappenglück, M.A., Ernstson, K., Mayer, W., Neumair, A., Sudhaus, D., and Liritzis, I., 2010. The fall of Phaethon: a Greco-Roman geomyth preserves the memory of a meteorite impact in Bavaria (south-east Germany). *Antiquity*, 84: 428–439.
- Rappenglück MA, Bauer F, Ernstson K, and Hiltl M. (2014) Meteorite impact on a micrometer scale: iron silicide, carbide and CAI minerals from the Chiemgau impact event (Germany). In: Problems and perspectives of modern mineralogy (Yushkin Memorial Seminar–2014) Proceedings, Syktyvkar, Komi Republic, Russia 19–22 May 2014, Syktyvkar, pp. 106-107.
- Rappenglück, M.A., Bauer, F., Hiltl, M., Neumair, A., and Ernstson, K., 2013. Calcium-Aluminum-rich Inclusions (CAIs) in iron silicide matter (Xifengite, Gupeite, Hapkeite): evidence of a cosmic origin. 76th Annual Meteoritical Society Meeting, *Meteor. Planet. Sci.* 48, s1, Abstract #5055.
- Rietmeijer, F.J.M., and Rotundi, A., 2005. Natural carbynes, including chaoite, on Earth, in meteorites, comets, circumstellar and interstellar dust. In: Cataldo, F. (ed.), *Polyynes: Synthesis, properties, and applications*. Boca Raton: CRC Press, 339–370.
- Robertson, L., 2002. Diamond-like amorphous carbon. *Materials Science and Engineering*, R37: 129–281.
- Rösler, W., Hoffmann, V., Raeymaekers, B., Schryvers, D., and Popp, J., 2005. Diamonds in carbon spherules – evidence for a cosmic impact? *Meteor. Planet. Sci.* 40: A129.
- Rösler, W., Patzelt, A., and Hoffmann, V., and Raeymaekers, B., 2006. *Characterisation of a small crater-like structure in SE Bavaria, Germany*. Abstract, European Space Agency, First International Conference on Impact Cratering in the Solar System, ESTEC, Noordwijk, The Netherlands, 08 – 12 May.
- Schüssler, U., Rappenglück, M.A., Ernstson, K., Mayer, W., and Rappenglück, B., 2005. Das Impakt-Kraterstrefefeld im Chiemgau. *Eur. J. Mineral.* 17, Beih. 1: 124.
- Schultz, P.H., Scott, H.R., Clemett, S.J., Thomas-Keprta, K.L., and Zárate, M., 2014. Preserved flora and organics in impact melt breccias. *Geology*, 42: 515–518.
- Shumilova, T.G., 2003. *Mineralogy of native carbon*. Ekaterinburg: UB RAS Press, 316 (in Russian).
- Shumilova, T.G., Danilova, Yu.V., Gorbunov, M.V., and Isaenko, S.I., 2011. Natural monocrystalline α -carbyne. *Doklady Earth Sciences*, 436(1): 152–154.
- Shumilova, T.G., Isaenko, S.I., Ulyashev, V.V., Kazakov, V.A., and Makeev, B.A., 2018. After-coal diamonds: an enigmatic type of impact diamonds. *Eur. J. Min.* 30: 61–76.
- Stöffler, D., and Langenhorst, F., 1994. Shock metamorphism of quartz in nature and experiment: I. Basic observation and theory. *Meteoritics*, 29: 155–181.
- Tagami, M., Liang, Y., Naito, H., Kawazoe, Y., and Kotani, M., 2014. Negatively curved cubic carbon crystals with octahedral symmetry. *Carbon*, 76: 266–274.
- Terrones, H., Terrones, M., Hernández, E., Grobert, N., Charlier, J.C., and Ajayan, P.M., 2000. New metallic allotropes of planar and tubular carbon. *Phys. Rev. Lett.*, 84(8): 1716–1719.
- Ulyashev, V.V., and Veligzhanin, 2016. AA Phase variety of carbon substance in the Kara impact structure by the data of synchrotron study. In: *Problems and perspectives of modern mineralogy* (Yushkin Memorial Seminar–2016). Syktyvkar, Komi Republic, Russia 17–20 May 2016, Proceedings. Syktyvkar Geoprint, 111-112 (in Russian).
- Wasson, J.T., 2003. Large aerial bursts; an important class of terrestrial accretionary events. *Astrobiology*, 3(1): 163–179.
- Wei, Q., Sankar, J., Sharma, A.K., Oktyabrsky, S., Narayan, J., and Narayan, R.J., 2000. Atomic structure, electrical properties, and infrared range optical properties of diamondlike carbon films containing foreign atoms prepared by pulsed laser deposition. *J. Materials Res.*, 15 (3): 633–641.
- Whittaker, A.G., 1979. Carbon: occurrence of carbyne forms of carbon in natural graphite. *Carbon*, 17(1): 21–24
- Wu Yingzhong, Duan Yi, Zhao Yang, Cao Xixi, Ma Lanhua, Qian Yaorong, Li Zhongping and Xing Lantian, 2018. Comparative study of hydrogen and carbon isotopic

- composition of gases generated from the pyrolysis of a peat under saltwater and freshwater conditions. *Acta Geologica Sinica* (English Edition) 92(5): 1879–1887.
- Yang, Z.Q., Verbeeck, J., Schryvers, D., Tarcea, N., Popp, J., and Rösler, W., 2008. TEM and Raman characterisation of diamond micro- and nanostructures in carbon spherules from upper soils. *Diamond & Related Materials*, 17: 937–943.
- Yezerkiy, V.A., 1982. Impactly metamorphosed coal substance in impactites. *Meteoritika*, 41: 134–140 (in Russian)
- Yezerkiy, V.A., 1986. High pressure polymorphs produced by the shock transformation of coals. *Intern. Geol. Rev.*, 28: 221–228. DOI:10.1080/00206818609466264.
- Zhuang, X., Chen, S., Zhang, T., Pan, X., Jiang, Y., and Bai, M., 2009. Thermal analysis on the combustion characteristics of seven kinds of biomass charcoals. *Chemistry and Industry of Forest Products* 29, Suppl., 0253 - 2417, SO- 0169 - 06 (in

Chinese).

About the first author

Tatyana SHUMILOVA, female, born in Vorkuta, Russian Federation, in December 1967. She received her PhD at the Institute of Geology UB Komi SC UB RAS in 1995. She was habilitated at the Saint-Petersburg Mining University (Leningrad Mining Institute) in 2003. At present she is a head of the Laboratory of Diamond Mineralogy and main scientist at the Institute of Geology UB Komi SC UB RAS and Affiliated Researcher at the University of Hawaii. She published over 50 papers in peer-reviewed journals such as *Scientific Reports*, *Carbon*, *European Journal of Mineralogy*, *Mineralogy and Petrology*, *Doklady Earth Sciences* and others.